depends on the relative expression of the transcriptional regulators T-bet and GATA3 (Szabo et al., 2000; Zheng and Flavell, 1997). Therefore, we examined the expression of T-bet and GATA3 in Th1- or Th2-skewing conditions. As previously reported (Szabo et al., 2000), high levels of T-bet mRNA expression were observed in Th1-conditioned cells of wild-type mice. However, the induction of T-bet expression was significantly impaired in Th1-conditioned cells of Sema4A-deficient mice (Figure 4D, upper). Consistent with this, the induction of IL-12 receptor β2 (IL-12Rβ2) in Th1-conditioned cells of Sema4A-deficient mice was significantly reduced compared to that of wild-type mice (Figure 4E). Conversely, although the expression of GATA3 was almost completely suppressed in Th1-conditioned cells of wild-type mice, substantial levels of GATA3 expression still remained in Th1-condtioned cells of Sema4A-deficient mice (Figure 4D, lower). When cells were cultured in Th2-skewing conditions, high levels of GATA3 expression were observed in both wild-type and Sema4A-deficient T cells (Figure 4D, lower). When Sema4A-Fc was included in the cultures of Th1-skewing conditions, the induction of T-bet expression and IFN-γ production were restored in Sema4A-deficient T cells (Figure 4D, upper, and Figure 4F). Collectively, these findings suggest that T cell-derived Sema4A is critically involved in the expression of T-bet and Th1 differentiation.

In Vivo T Cell Priming in Sema4A-Deficient Mice

We next examined the effects of Sema4A deficiency on in vivo T cell activation. Wild-type or Sema4A-deficient mice were immunized with keyhole limpet haemocyanin (KLH) in complete Freund's adjuvant (CFA) into the hind footpad. Five days after immunization, $CD4^+$ T cells were prepared from the draining lymph nodes of the immunized mice and tested in vitro for antigen-specific responses. As shown in Figure 5A, $CD4^+$ T cell responses to KLH were considerably reduced in Sema4A-deficient mice compared to wild-type mice. In particular, the production of IFN-γ in response to KLH was markedly impaired, while the reduction in IL-4 production was not as substantial. We next examined in vivo T cell responses by immunizing mice with KLH in alum. Seven days after immunization, $CD4^+$ T cells were prepared from the draining lymph nodes and restimulated with KLH in vitro. As shown in Figure 5B, IL-4 production in response to KLH was enhanced in Sema4A-deficient mice, but IFN-γ production was reduced. Collectively, these results suggest that Sema4A is involved in both the generation of antigen-specific T cells as well as playing a role in in vivo Th1/Th2 differentiation.

Reduced Th1 Responses in Sema4A-Deficient Mice

To explore the influence of Sema4A deficiency on in vivo antibody responses, Sema4A-deficient mice were immunized with a TD antigen, 4-hydroxy-3-nitrophenylacetyl-chicken-γ-globulin conjugate (NP-CGG). Sema4A-deficient mice displayed impaired anti-NP antibody responses (Figure 5C). In particular, IgG2b and IgG3 responses, known to reflect Th1 responses, were significantly impaired. Antibody responses in IgG1, an isotype related to Th2 responses, were not significantly affected by Sema4A deficiency. In addition, antibody responses against T cell-independent (TI) antigens such as TNP-LPS and NP-Ficoll were normal (data not shown).

We further investigated a role of Sema4A in in vivo Th1 and Th2 responses in greater detail by using several immunization and infection systems. Wild-type and Sema4A-deficient mice were intraperitoneally injected with *Propionibacterium acnes* (*P. acnes*), an agent known to induce Th1 responses. Seven or 14 days after injection, $CD4^+$ T cells were purified from splenocytes and stimulated with immobilized anti-CD3. Elevated levels of IFN-γ were observed in wild-type mice, whereas IFN-γ production from Sema4A-deficient T cells did not increase above basal levels (Figure 6A). We next utilized a delayed-type hypersensitivity (DTH) model. Wild-type and Sema4A-deficient mice were immunized with OVA. Seven days after immunization, the mice were challenged with OVA into the hind footpad, and footpad swelling was measured. As shown in Figure 6B, Sema4A-deficient mice exhibited impaired DTH responses compared to those observed in wild-type mice. These results indicate that the in vivo Th1 responses are impaired in Sema4A-deficient mice.

We further investigated Th2 development in vivo by infecting mice with the intestinal parasitic nematode, *Nippostrongylus brasiliensis* (*N. brasiliensis*), which is known to induce Th2 responses (Takeda et al., 1996). Eight days after infection, splenic $CD4^+$ T cells from *N. brasiliensis*-infected wild-type and Sema4A-deficient mice were stimulated with immobilized anti-CD3 mAb for 24 hr, and the culture supernatants were analyzed for IL-4 production. As shown in Figure 6C, enhanced production of IL-4 was observed in Sema4A-deficient mice. However, IFN-γ production in *N. brasiliensis*-infected Sema4A-deficient mice was comparable to that in *N. brasiliensis*-infected wild-type mice (data not shown). Furthermore, the elevation of serum IgE levels were considerably accelerated in Sema4A-deficient mice compared to those seen in wild-type mice (Figure 6C). Collectively, these results suggest that Sema4A is involved in regulating in vivo Th2 responses.

Involvement of DC-Derived and T Cell-Derived Sema4A in Different Phases of the Immune Responses

The expression of Sema4A on both DCs and Th1-differentiating cells suggests that DC-derived and T cell-derived Sema4A may play distinct roles at different phases of the immune responses. In order to address this question, we performed a reconstitution experiment by transferring antigen-pulsed wild-type or Sema4A-deficient DCs into wild-type or Sema4A-deficient mice. Seven days after injection, $CD4^+$ T cells were purified from the spleen and restimulated with KLH (Figure 7A). When wild-type DCs were injected into wild-type mice, antigen-specific T cell responses were markedly induced. In contrast, when Sema4A-deficient DCs were injected into Sema4A-deficient mice, antigen-specific T cell responses were considerably impaired. Interestingly, the injection of Sema4A-deficient DCs into either wild-type or Sema4A-deficient mice resulted in impaired proliferation and IL-2 production, showing the

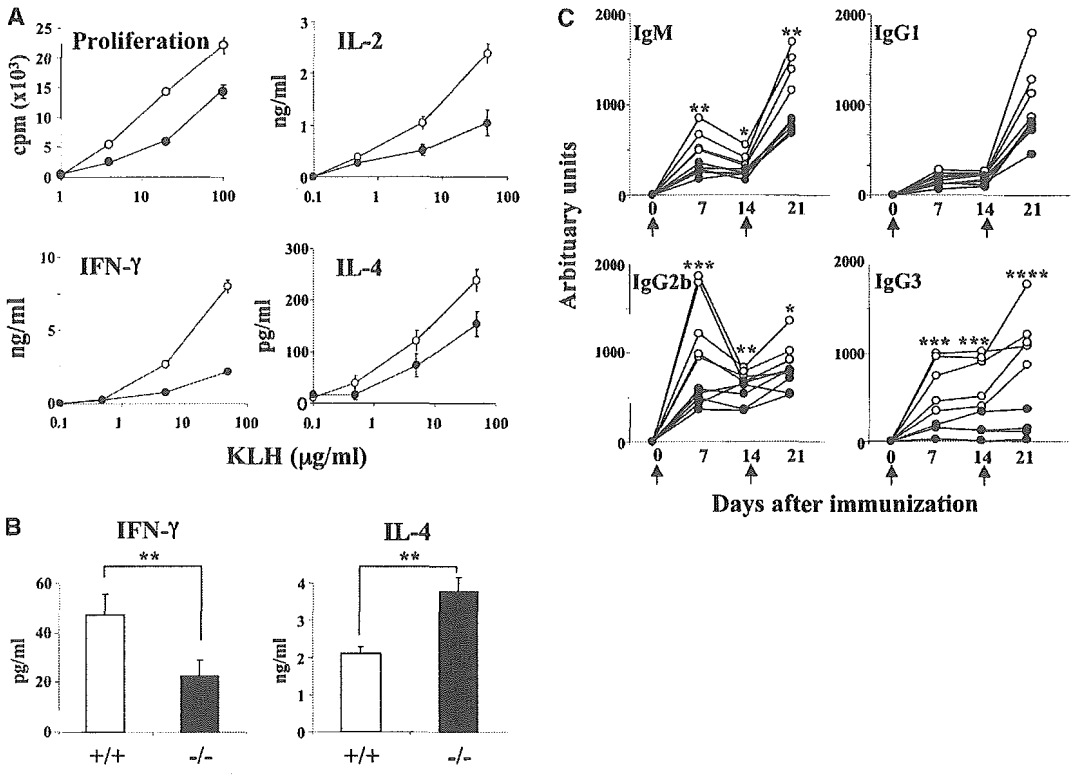

Figure 5. Impaired Antigen-Specific T Cell Priming and Antibody Responses in Sema4A-Deficient Mice

(A) Impaired T cell priming in Sema4A-deficient mice. Wild-type (open circles) and Sema4A-deficient mice (closed circles) were immunized with KLH in CFA into the hind footpad. Five days after priming, $CD4^+$ T cells prepared from the draining lymph nodes were restimulated with various concentrations of KLH. Cells were examined for proliferation and cytokine production.

(B) Enhanced IL-4 production in Sema4A-deficient mice. Wild-type (open bars) and Sema4A-deficient mice (closed bars) were immunized with KLH in alum. Seven days after priming, $CD4^+$ T cells prepared from the draining lymph nodes were restimulated with KLH, and cytokine production was examined.

(C) Impaired TD responses in Sema4A-deficient mice. Wild-type (open circles; n = 5) and Sema4A-deficient (closed circles; n = 5) mice (8–12 weeks old) were immunized intraperitoneally with 100 μg NP-CGG as an alum-precipitated complex on day 0 and 14 (arrows) and were bled at the indicated times. Levels of anti-NP antibodies were determined by using ELISA plates coated with NP_{12}-conjugated BSA. The results shown are representative of two independent experiments. *, $p < 0.05$; **, $p < 0.01$; ***, $p < 0.005$, ****, $p < 0.001$.

Error bars indicate mean ± SD.

importance of DC-derived Sema4A in T cell priming. Conversely, the injection of wild-type DCs into Sema4A-deficient mice, in which the T cells lack Sema4A, led to significantly reduced IFN-γ production but enhanced IL-4 production, suggesting the involvement of T cell-derived Sema4A in Th1 responses. Similarly, when DCs were pulsed with *P. acnes*, a potent Th1-inducing agent, the injection of wild-type DCs into Sema4A-deficient mice also led to severely impaired IFN-γ production (Figure 7B), of which impairment could be restored by administration of soluble Sema4A protein (Figure S4). Thus, DC- and T cell-derived Sema4A play distinct roles in the development of an immune response.

Discussion

Nonredundant Roles of Sema4A in the Immune System Revealed by Gene Targeting

Sema4A-deficient mice developed normally and were fertile, although Sema4A is expressed in a broad range of tissues from embryogenesis to adulthood (Kumanogoh et al., 2002a; Puschel et al., 1995). Our present study has revealed the functional defects of Sema4A-deficient mice in the immune system. In vitro analysis showed that Sema4A-deficient DCs poorly stimulated allogeneic T cells, and Sema4A-deficient T cells displayed defective Th differentiation. In addition, in vivo studies revealed that humoral and cellular immune responses were defective in Sema4A-deficient mice. Collectively, these results indicate that Sema4A plays nonredundant roles in the immune system. However, there are several possibilities for our failure to detect defects in systems other than the immune system. First, Sema4A may not be essential for the development of nonlymphoid tissues. Second, other family members outside the immune system could compensate for the absence of Sema4A. In this case, receptors for Sema4A, including Tim-2, might have additional ligands outside the immune system. Indeed, semaphorin receptors like neuropilins and plexins are known to be shared by several semaphorin family members (He and Tessier-Lavigne, 1997; Kolodkin et al., 1997; Kumanogoh et al., 2000; Pasterkamp et al., 2003; Shi et al.,

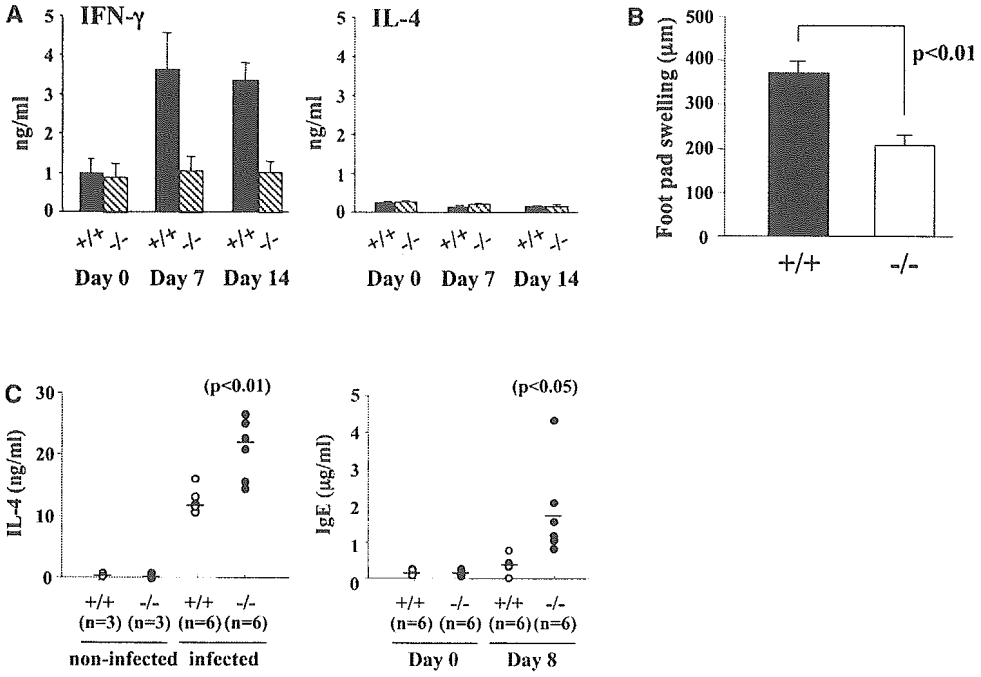

Figure 6. Defective Th1/Th2 Regulation in Sema4A-Deficient Mice

(A) Th1 responses induced by *P. acnes*. Wild-type (black bars) and Sema4A-deficient mice (hatched bars) were intraperitoneally injected with 200 μg heat-killed *P. acnes*. Seven days after injection, $CD4^+$ T cells from the spleen were stimulated with anti-CD3 for 24 hr. The concentrations of IFN-γ and IL-4 in the culture supernatants were measured by ELISA.

(B) DTH responses in Sema4A-deficient mice. Wild-type (black bars) and Sema4A-deficient (white bars) mice were immunized with OVA in CFA. Seven days later, mice were challenged in the footpad with OVA, and footpad swelling was measured 2 days after challenge.

(C) Enhanced Th2 Responses to *N. brasliensis* in Sema4A-Deficient Mice. (left) IL-4 production in response to *N. brasliensis* infection. Splenic $CD4^+$ T cells from wild-type (open circles) or Sema4A-deficient (closed circles) mice were prepared from mice infected with the suboptimal doses of *N. brasliensis*. Cells were stimulated with immobilized anti-CD3 for 24 hr. Supernatants were analyzed by ELISA. (right) IgE responses in *N. brasliensis* infection. Serum IgE levels of wild-type (open circles) or Sema4A-deficient (closed circles) mice were measured at day 0 and day 8 after the infection by using a mouse IgE ELISA kit.

Error bars indicate mean ± SD.

2000; Kumanogoh and Kikutani, 2003; Toyofuku et al., 2004), suggesting the existence of functional redundancy. Alternatively, the mutant mice may have subtle defects that were overlooked in our preliminary analyses. In this case, further examination of the mutant mice will be required.

Requirement of Sema4A on DCs for T Cell Activation

We found that the allostimulatory activities of DCs were significantly impaired in Sema4A-deificient mice. Sema4A expression on activated T cells was not critically involved in MLRs. The expression levels of costimulatory molecules on Sema4A-deficient DCs were comparable to those on wild-type DCs. It thus appears that the deficiency of Sema4A on DCs is primarily responsible for the impaired activity of DCs to stimulate allogeneic T cells. In this context, the reduced stimulatory activities of Sema4A-deficient DCs could explain the defective T cell priming in Sema4A-deficient mice. Indeed, these results are consistent with the previous findings with recombinant soluble Sema4A or anti-Sema4A mAb (Kumanogoh et al., 2002a), that is, soluble Sema4A proteins enhanced the MLR by directly acting on T cells, while anti-Sema4A mAb inhibited the MLR. Also, it has been previously shown that in vivo administration of soluble Sema4A proteins promotes T cell priming, whereas anti-Sema4A mAb inhibits the generation of antigen-specific T cells. Furthermore, the reconstitution experiment performed in this study also supports the critical role of DC-derived Sema4A in T cell activation.

Requirement of T Cell-Derived Sema4A for T Cell Differentiation

Although the expression of Sema4A has been shown to be inducible on activated T cells (Kumanogoh et al., 2002a), the functional significance of T cell-derived Sema4A was not previously identified. We here showed that the levels of Sema4A expression on T cells were significantly and selectively enhanced throughout Th1 differentiation, but not Th2 differentiation. Moreover, we performed a series of in vitro T cell differentiation experiments that did not include APCs, and we demonstrated a role for T cell-derived Sema4A in T cell responses, in particular, Th1 differentiation. In vitro differentiation of Sema4A-deficient T cells into Th1 cells was severely impaired, while differentiation into Th2 cells was only slightly affected. These observations strongly suggest that increased expression of Sema4A on Th1-differentiating cells can further promote Th1 dif-

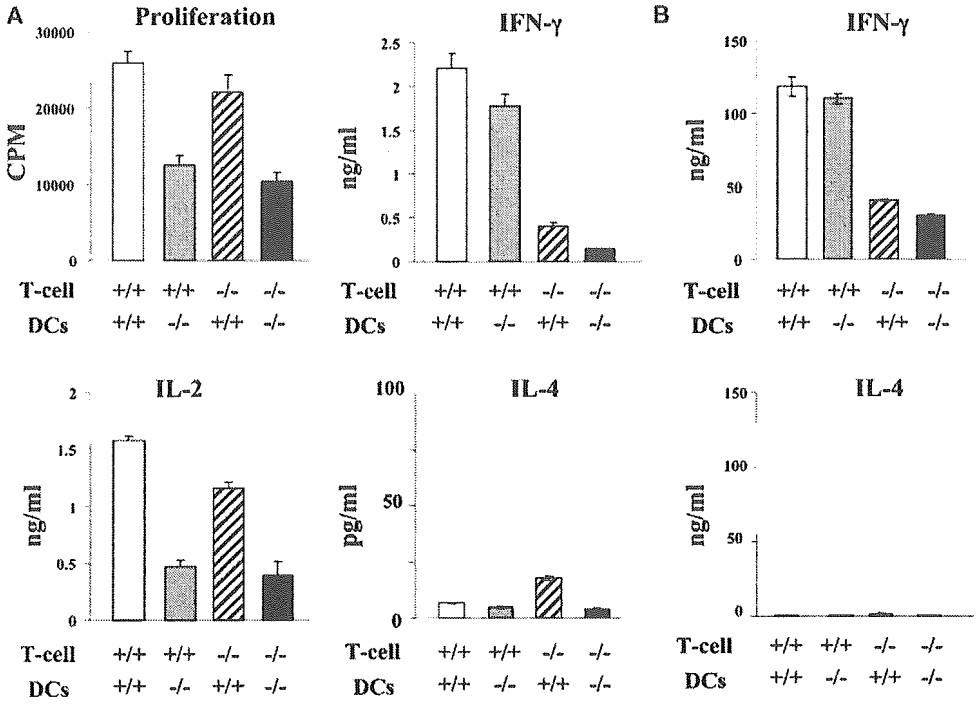

Figure 7. Transfer of Antigen-Pulsed DCs into Sema4A-Deficient Mice

(A) Involvement of DC-derived Sema4A and T cell-derived Sema4A in distinct phases of immune responses. Sema4A-deficient or wild-type DCs pulsed with KLH were injected into wild-type or Sema4A-deficient mice. Seven days after DC injection, $CD4^+$ T cells purified from the spleen were restimulated with KLH for 72 hr.

(B) Involvement of T cell-derived Sema4A in *P. acnes*-induced Th1 responses. Sema4A-deficient or wild-type DCs pulsed with *P. acnes* were injected into wild-type or Sema4A-deficient mice. Seven days after DC injection, $CD4^+$ T cells purified from the spleen were restimulated with *P. acnes* for 72 hr. For proliferation assays, cells were pulsed with 2 μCi [^{3}H]-thymidine for the last 14 hr. Levels of cytokines in the culture supernatants were measured by using the Bio-Plex suspension array system.

ferentiation. Under these circumstances, Sema4A might function in an autocrine manner or through cognate T cell-T cell contacts. Collectively, the present findings identified a function for T cell-derived Sema4A in addition to that of DC-derived Sema4A.

The induction of T-bet was severely impaired in Sema4A-deficient T cells under Th1-skewing conditions. T-bet is a Th1-specific transcriptional factor crucial for commitment to Th1 lineage (Szabo et al., 2000; Hatton and Weaver, 2003). This underscores the importance of Sema4A in Th1 differentiation. Indeed, ectopic expression of T-bet by retrovirus restored the Th1 polarization of Sema4A-deficient T cells (Figure S5). In this context, Sema4A deficiency may affect T-bet expression or signals responsible for its expression. Of note, the induction of IL-12Rβ2, which is crucially dependent on T-bet (Afkarian et al., 2002), was significantly reduced in Th1-conditioned cells of Sema4A-deficient mice compared to wild-type mice (Figure 4E). Under Th1-skewing conditions, Sema4A-deficient T cells displayed rather poor responses to IL-12 compared to IFN-γ (Figure S6). In this context, the poor IL-12 responsiveness of Sema4A-deficient T cells might be critical for the impaired Th1 differentiation. Further studies are required to elucidate the mechanism by which Sema4A is involved in regulating T-bet induction during Th1 differentiation.

After differentiated into Th1 cells in the presence of Sema4A-Fc, Sema4A-deficient cells could produce almost normal levels of IFN-γ in response to anti-CD3 even without exogenous Sema4A (Figure 4F). This finding suggests that Sema4A is necessary for Th1 differentiation, but not for the functions of Th1 effector cells. However, we cannot exclude the possibility that high levels of Sema4A expression on Th1-polarized cells may have unidentified functions.

Involvement of Sema4A in Regulating Th1/Th2 Responses

Immunization with protein antigens led to significantly reduced in vivo T cell responses in Sema4A-deficient mice. This may reflect roles of Sema4A in both antigen-specific T cell priming and Th1 differentiation. Sema4A is constitutively and abundantly expressed on the cell surface of DCs. Furthermore, Sema4A-deficient DCs displayed a significantly reduced ability to stimulate allogeneic T cells. These findings suggest that DC-derived Sema4A is involved in the early phase of T cell activation, which is crucial for T cell priming. In vitro proliferation of Sema4A-deficient T cells in response to anti-CD3 was slightly reduced, suggesting that T cell-derived Sema4A may be also relevant to T cell activation. At the moment, we do not know to what extent T cell-derived Sema4A is involved in the early phases of T cell activation. In addition to the defects in the generation of antigen-specific T cells, Sema4A-deficient mice displayed severely impaired Th1 responses upon

immunization with protein antigens. Also in *P. acnes* and DTH models, we observed that Th1 responses were impaired in Sema4A-deficient mice. These defects seem to be consistent with impaired in vitro Th1 differentiation of Sema4A-deficient T cells. Similarly, Sema4A-deficient mice exhibited impaired antibody responses not only in IgM, but also in IgG2b and IgG3, isotypes promoted during Th1 responses. It therefore appears that Sema4A may promote conditions favorable for Th1 differentiation. Sema4A, of which high levels of expression are increasingly induced on Th1-differentiating cells, might be involved in a relatively late phase of T cell responses, in particular, Th1 differentiation. The impaired T cell responses seen in Sema4A-deficient mice reconstituted with wild-type antigen-pulsed DCs strongly support the functional significance of T cell-derived Sema4A in in vivo Th1 responses.

In contrast to the in vivo Th1 responses, in vivo Th2 responses seem to be enhanced in Sema4A-deficient mice. In *N. brasiliensis* infection, Th2 responses, including IL-4 production and serum IgE levels, were substantially promoted in the mutant mice compared to those in wild-type mice. Upon infection with live nematodes that may overcome impaired T cell priming, defective Th1 responses might in turn lead to enhanced Th2 responses in Sema4A-deficient mice. It is also possible that the reduction in T-bet might lead to an imbalance between Th1 and Th2. Indeed, it has been shown that T-bet-deficient mice exhibit not only impaired Th1 responses, but also enhanced Th2 responses, the latter of which includes spontaneously developed multiple physiologic and inflammatory features characteristic of asthma (Finotto et al., 2002). In this context, the impaired induction of T-bet in Sema4A-deficient T cells might explain why Sema4A-deficient mice exhibited defective in vivo Th1 responses but enhanced in vivo Th2 responses.

Tim-2 is involved in Sema4A-mediated T cell activation (Kumanogoh et al., 2002a). Here, we found that the expression of Tim-2 is inducible not only in activated T cells, but also in Th-differentiated cells (Figure S2). Although it appears that Tim-2 has some role in Sema4A-mediated Th1 differentiation (Figure S7), we have not still reached the definitive conclusion about a role of Tim-2 for Sema4A-mediated Th1 differentiation. In addition, we cannot exclude a possibility that Sema4A might have distinct receptors to exert its different effects during T cell activation and differentiation. Of note, many members of the semaphorin family, including class IV semaphorins, play developmental roles through plexins in various embryonic tissues (Tamagnone and Comoglio, 2000). Indeed, we have recently found that Sema4A can also bind some members of the plexin family (T.T. et al., unpublished data), which fact suggests a possibility that some plexins may also be involved in Sema4A signaling in the immune system. Further studies would be required to determine how Sema4A functions in distinct phases of immune responses.

In conclusion, we have demonstrated nonredundant roles of Sema4A in the immune system, not only confirming a function of DC-derived Sema4A in T cell activation, but also revealing a role for T cell-derived Sema4A, especially for Th1 differentiation. As a consequence, Sema4A deficiency profoundly affected in vivo T cell responses. The present findings provide not only new insight into the regulation of Th1/Th2 responses, but also a clue for the potentiation of and intervention in pathological immune responses.

Experimental Procedures

Gene Targeting

Generation of Sema4A-deficient mice was described in the Supplemental Experimental Procedures. All experimental procedures were consistent with institutional guidelines.

Flow Cytometric Analysis and Antibodies

One million cells from the various tissues tested were stained with the following antibodies: anti-CD4 (GK1.5), anti-CD62L (MEL-14), anti-CD11c (HL3), anti-B220 (RA3-6B2), anti-CD40 (3/23), anti-CD80 (16-10A1), anti-CD86 (GL-1), anti-I-A^b (25-9-17), anti-CD45.1 (Ly5.1), and anti-Sema4A (SK31, 5E3) (Kumanogoh et al., 2002a) conjugated with FITC, phycoerythrin (PE), or biotin in the presence or absence of Fc block (anti-CD16/32, 2.4G2). Streptavidin-FITC, -PE, and -allophycocyanin (APC) were used as second-step reagents for biotinylated antibodies. These antibodies and reagents, except for anti-Sema4A, were purchased from Pharmingen (Kumanogoh et al., 2002a). An anti-Sema4A mAb (5E3) was established by immunizing Sema4A-deficient mice with Sema4A-Fc proteins. Analysis of intracellular cytokines was performed according to the manufacturer's protocol (Pharmingen). Cells were stained with the following monoclonal antibodies (Pharmingen): PE-conjugated anti-IL-4 (1D11), FITC-conjugated anti-IFN-γ (XMG1.2), and isotype controls. Data analysis was performed by using FlowJo software (Treestar).

In Vitro Assays

B cells and T cells were isolated from the spleen or lymph nodes by using MACS sorting (Miltenyi Biotech, Germany). The resulting purity was >95% in each experiment. DCs were generated from the bone marrow progenitors of wild-type or Sema4A-deficient mice by using GM-CSF as previously described (Inaba et al., 1992; Kumanogoh et al., 2002b). For in vitro T cell differentiation assays, $CD62L^{high}$ $CD4^+$ naïve T cells were purified by using FACS sorting as described previously (Kumanogoh et al., 2001; Kumanogoh et al., 2002a). $CD62L^{high}$ $CD4^+$ naïve T cells (1×10^5 cells/ml) prepared from wild-type or Sema4A-deficient mice were cultured with immobilized anti-CD3 (0.1, 1, 2, 10 μg/ml) plus anti-CD28 mAbs (10 μg/ml) in the presence of IL-12 (1, 10, 100 U/ml) plus anti-IL-4 (10 μg/ml) (Th1-skewing conditions) or in the presence of IL-4 (1, 10, 100 U/ml) plus anti-IL-12 (10 μg/ml) and anti-IFN-γ (10 μg/ml) (Th2-skewing conditions) with or without Sema4A-Fc (10 μg/ml) (Kumanogoh et al., 2002a). For B cell proliferation assays, 1×10^5 purified B cells were cultured for 72 hr with or without various concentrations of anti-CD40 mAb (HM40-3), LPS (Sigma), or anti-μ in 96-well microtiterplates. For T cell proliferation assays, 2×10^4 cells were cultured with or without immobilized anti-CD3 (2C11) and anti-CD28 (37.51) for 48 hr in 96-well microtiterplates. For IL-12 production assays, the concentration of IL-12 in the culture supernatants was measured after culturing DCs (1×10^5 cells/ml) for 72 hr with or without anti-CD40 (3/23) or LPS. The IL-12 was detected by using a mouse IL-12p40 ELISA kit (R&D Systems). For MLRs, $CD4^+$ T cells (5×10^4 cells/well) were cultured with irradiated (3000 rad) allogeneic DCs for 48 hr. Bone marrow-derived DCs were pretreated with anti-CD40 for 24 hr. To measure cell proliferation, cells were pulsed with 2 μCi [^{3}H]-thymidine for the last 14 hr of the culture period.

T Cell Priming

Mice were immunized with 10 μg KLH in CFA into the hind footpads. Five days after priming, $CD4^+$ T cells were purified from the draining lymph nodes by MACS, and 5×10^4 cells were stimulated for 72 hr with various concentrations of KLH in the presence of irradiated (3000 rad) splenocytes (2.5×10^5) of wild-type littermates. For KLH immunization in alum, mice were immunized with 50 μg KLH in alum into the hind footpads. Seven days after the immunization, $CD4^+$ T cells were purified from the draining lymph nodes by MACS, and 5×10^4 cells were stimulated for 72 hr with

KLH in the presence of irradiated (3000 rad) splenocytes (2.5×10^5) of wild-type littermates.

For proliferation assays, cells were pulsed with 2 μCi [^{3}H]-thymidine for the last 14 hr. Levels of cytokines in the culture supernatants were measured by using ELISA kits (R&D systems).

Immunization and Antibody Assays

To induce antibody responses to TD antigen, 8-week-old mice were immunized intraperitoneally with 100 μg NP-CGG as an alum-precipitated complex at day 0 and boosted at day 14. NP-specific antibodies were detected with NP_{12}-BSA-coated ELISA plates and quantified by isotype-specific ELISA as described (Shi et al., 2000).

In Vivo Induction of Th1/Th2 Responses

Mice were injected intraperitoneally with 200 μg heat-killed *P. acnes* to induce Th1 responses in vivo. Seven or 14 days after injection, splenic CD4$^+$ T cells were purified and stimulated on immobilized anti-CD3-coated plates for 24 hr as described previously (Takeda et al., 1998). For DTH, wild-type and Sema4A-deficient mice were immunized subcutaneously with OVA in CFA (Chen et al., 1999). Seven days later, mice were challenged in the footpad with OVA, and footpad swelling was measured 2 days after challenge.

For *N. brasiliensis* infection, 400 third-stage *N. brasiliensis* larvae were injected subcutaneously into Sema4A-deficient and wild-type mice. Eight days after the infection, CD4$^+$ T cells were purified from the splenocytes and cultured with immobilized anti-CD3 for 24 hr. Levels of IFN-γ and IL-4 in culture supernatants and serum levels of IgE were measured by ELISA.

Transfer Experiment

DCs were generated from bone marrow cultured in the presence of GM-CSF as described previously (Inaba et al., 1992). DCs were pulsed with KLH (50 μg/ml) in the presence of anti-CD40 (0.2 μg/ml) or *P. acnes* (10 μg/ml) for 24 hr. For in vivo transfer experiments, mice were injected i.p. with 1×10^6 antigen-pulsed DCs as previously described (MacDonald et al., 2002). Seven days after DC injection, CD4$^+$ T cells were purified from the spleen and stimulated with KLH (20 μg/ml) or *P. acnes* (5 μg/ml) in the presence of irradiated (3000 rad) Thy1$^+$-depleted spleen cells of wild-type littermates for 72 hr. For proliferation assays, cells were pulsed with 2 μCi [^{3}H]-thymidine for the last 14 hr. Levels of cytokines in the culture supernatants were measured by using Bio-Plex suspension array system (Bio-Rad).

Supplemental Data

Supplemental Data including Experimental Procedures, one table, and seven figures are available at http://www.immunity.com/cgi/content/full/22/3/305/DC1/.

Acknowledgments

We thank Ms. K. Kubota for excellent secretarial assistance. We also thank Y. Maruyama, A. Kawai, J. Yoshida, K. Shiozaki, N. Okita, N. Iwami, and K. Nakamura for technical support. We are grateful to Drs. K. Nakanishi, P. Rennert, M. Fujimoto, S. Habu, H. Arase, T. Kitamura, T. Kurosaki, T. Kaisho, and K. Hoshino for providing materials, critical advice, and discussion. This study was supported by research grants from the Ministry of Education, Culture, Sports, Science, and Technology, Japan and from the Core Research for Evolutional Science and Technology program of the Japan Science and Technology Agency to A.K. and H.K.

Received: June 24, 2004
Revised: January 11, 2005
Accepted: January 17, 2005
Published: March 22, 2005

References

Afkarian, M., Sedy, J.R., Yang, J., Jacobson, N.G., Cereb, N., Yang, S.Y., Murphy, T.L., and Murphy, K.M. (2002). T-bet is a STAT1-induced regulator of IL-12R expression in naive CD4+ T cells. Nat. Immunol. *3*, 549–557.

Chae, S.C., Song, J.H., Lee, Y.C., Kim, J.W., and Chung, H.T. (2003). The association of the exon 4 variations of Tim-1 gene with allergic diseases in a Korean population. Biochem. Biophys. Res. Commun. *312*, 346–350.

Chen, A.I., McAdam, A.J., Buhlmann, J.E., Scott, S., Lupher, M.L., Jr., Greenfield, E.A., Baum, P.R., Fanslow, W.C., Calderhead, D.M., Freeman, G.J., and Sharpe, A.H. (1999). Ox40-ligand has a critical costimulatory role in dendritic cell:T cell interactions. Immunity *11*, 689–698.

Finotto, S., Neurath, M.F., Glickman, J.N., Qin, S., Lehr, H.A., Green, F.H., Ackerman, K., Haley, K., Galle, P.R., Szabo, S.J., et al. (2002). Development of spontaneous airway changes consistent with human asthma in mice lacking T-bet. Science *295*, 336–338.

Hatton, R.D., and Weaver, C.T. (2003). Immunology. T-bet or not T-bet. Science *302*, 993–994.

He, Z., and Tessier-Lavigne, M. (1997). Neuropilin is a receptor for the axonal chemorepellent Semaphorin III. Cell *90*, 739–751.

Inaba, K., Inaba, M., Romani, N., Aya, H., Deguchi, M., Ikehara, S., Muramatsu, S., and Steinman, R.M. (1992). Generation of large numbers of dendritic cells from mouse bone marrow cultures supplemented with granulocyte/macrophage colony stimulating factor. J. Exp. Med. *176*, 1693–1702.

Kikutani, H., and Kumanogoh, A. (2003). Semaphorins in interactions between T cells and antigen-presenting cells. Nat. Rev. Immunol. *3*, 159–167.

Kolodkin, A.L., Matthes, D.J., and Goodman, C.S. (1993). The semaphorin genes encode a family of transmembrane and secreted growth cone guidance molecules. Cell *75*, 1389–1399.

Kolodkin, A.L., Levengood, D.V., Rowe, E.G., Tai, Y.T., Giger, R.J., and Ginty, D.D. (1997). Neuropilin is a semaphorin III receptor. Cell *90*, 753–762.

Kuchroo, V.K., Umetsu, D.T., DeKruyff, R.H., and Freeman, G.J. (2003). The TIM gene family: emerging roles in immunity and disease. Nat. Rev. Immunol. *3*, 454–462.

Kumanogoh, A., and Kikutani, H. (2003). Immune semaphorins: a new area of semaphorin research. J. Cell Sci. *116*, 3463–3470.

Kumanogoh, A., Watanabe, C., Lee, I., Wang, X., Shi, W., Araki, H., Hirata, H., Iwahori, K., Uchida, J., Yasui, T., et al. (2000). Identification of CD72 as a lymphocyte receptor for the class IV semaphorin CD100: a novel mechanism for regulating B cell signaling. Immunity *13*, 621–631.

Kumanogoh, A., Wang, X., Lee, I., Watanabe, C., Kamanaka, M., Shi, W., Yoshida, K., Sato, T., Habu, S., Itoh, M., et al. (2001). Increased T cell autoreactivity in the absence of CD40–CD40 ligand interactions: a role of CD40 in regulatory T cell development. J. Immunol. *166*, 353–360.

Kumanogoh, A., Marukawa, S., Suzuki, K., Takegahara, N., Watanabe, C., Ch'ng, E., Ishida, I., Fujimura, H., Sakoda, S., Yoshida, K., and Kikutani, H. (2002a). Class IV semaphorin Sema4A enhances T-cell activation and interacts with Tim-2. Nature *419*, 629–633.

Kumanogoh, A., Suzuki, K., Ch'ng, E., Watanabe, C., Marukawa, S., Takegahara, N., Ishida, I., Sato, T., Habu, S., Yoshida, K., et al. (2002b). Requirement for the lymphocyte semaphorin, CD100, in the induction of antigen-specific T cells and the maturation of dendritic cells. J. Immunol. *169*, 1175–1181.

MacDonald, A.S., Straw, A.D., Dalton, N.M., and Pearce, E.J. (2002). Th2 response induction by dendritic cells: a role for CD40. J. Immunol. *168*, 537–540.

McIntire, J.J., Umetsu, S.E., Akbari, O., Potter, M., Kuchroo, V.K., Barsh, G.S., Freeman, G.J., Umetsu, D.T., and DeKruyff, R.H. (2001). Identification of Tapr (an airway hyperreactivity regulatory locus) and the linked Tim gene family. Nat. Immunol. *2*, 1109–1116.

McIntire, J.J., Umetsu, S.E., Macaubas, C., Hoyte, E.G., Cinnioglu, C., Cavalli-Sforza, L.L., Barsh, G.S., Hallmayer, J.F., Underhill, P.A., Risch, N.J., et al. (2003). Immunology: hepatitis A virus link to atopic disease. Nature *425*, 576.

Monney, L., Sabatos, C.A., Gaglia, J.L., Ryu, A., Waldner, H., Chernova, T., Manning, S., Greenfield, E.A., Coyle, A.J., Sobel, R.A., et

al. (2002). Th1-specific cell surface protein Tim-3 regulates macrophage activation and severity of an autoimmune disease. Nature *415*, 536–541.

Pasterkamp, R.J., and Kolodkin, A.L. (2003). Semaphorin junction: making tracks toward neural connectivity. Curr. Opin. Neurobiol. *13*, 79–89.

Pasterkamp, R.J., Peschon, J.J., Spriggs, M.K., and Kolodkin, A.L. (2003). Semaphorin 7A promotes axon outgrowth through integrins and MAPKs. Nature *424*, 398–405.

Puschel, A.W., Adams, R.H., and Betz, H. (1995). Murine semaphorin D/collapsin is a member of a diverse gene family and creates domains inhibitory for axonal extension. Neuron *14*, 941–948.

Sabatos, C.A., Chakravarti, S., Cha, E., Schubart, A., Sanchez-Fueyo, A., Zheng, X.X., Coyle, A.J., Strom, T.B., Freeman, G.J., and Kuchroo, V.K. (2003). Interaction of Tim-3 and Tim-3 ligand regulates T helper type 1 responses and induction of peripheral tolerance. Nat. Immunol. *4*, 1102–1110.

Sanchez-Fueyo, A., Tian, J., Picarella, D., Domenig, C., Zheng, X.X., Sabatos, C.A., Manlongat, N., Bender, O., Kamradt, T., Kuchroo, V.K., et al. (2003). Tim-3 inhibits T helper type 1-mediated auto- and alloimmune responses and promotes immunological tolerance. Nat. Immunol. *4*, 1093–1101.

Shi, W., Kumanogoh, A., Watanabe, C., Uchida, J., Wang, X., Yasui, T., Yukawa, K., Ikawa, M., Okabe, M., Parnes, J.R., et al. (2000). The class IV semaphorin CD100 plays nonredundant roles in the immune system: defective B and T cell activation in CD100-deficient mice. Immunity *13*, 633–642.

Szabo, S.J., Kim, S.T., Costa, G.L., Zhang, X., Fathman, C.G., and Glimcher, L.H. (2000). A novel transcription factor, T-bet, directs Th1 lineage commitment. Cell *100*, 655–669.

Takeda, K., Tanaka, T., Shi, W., Matsumoto, M., Minami, M., Kashiwamura, S., Nakanishi, K., Yoshida, N., Kishimoto, T., and Akira, S. (1996). Essential role of Stat6 in IL-4 signalling. Nature *380*, 627–630.

Takeda, K., Tsutsui, H., Yoshimoto, T., Adachi, O., Yoshida, N., Kishimoto, T., Okamura, H., Nakanishi, K., and Akira, S. (1998). Defective NK cell activity and Th1 response in IL-18-deficient mice. Immunity *8*, 383–390.

Tamagnone, L., and Comoglio, P.M. (2000). Signalling by semaphorin receptors: cell guidance and beyond. Trends Cell Biol. *10*, 377–383.

Toyofuku, T., Zhang, H., Kumanogoh, A., Takegahara, N., Suto, F., Kamei, J., Aoki, K., Yabuki, M., Hori, M., Fujisawa, H., and Kikutani, H. (2004). Dual roles of Sema6D in cardiac morphogenesis through region-specific association of its receptor, Plexin-A1, with off-track and vascular endothelial growth factor receptor type 2. Genes Dev. *18*, 435–447.

Zheng, W., and Flavell, R.A. (1997). The transcription factor GATA-3 is necessary and sufficient for Th2 cytokine gene expression in CD4 T cells. Cell *89*, 587–596.

nature medicine

Role of STAT-3 in regulation of hepatic gluconeogenic genes and carbohydrate metabolism *in vivo*

Hiroshi Inoue[1], Wataru Ogawa[1], Michitaka Ozaki[2,3], Sanae Haga[2], Michihiro Matsumoto[1], Kensuke Furukawa[1], Naoko Hashimoto[1], Yoshiaki Kido[1], Toshiyuki Mori[1], Hiroshi Sakaue[1], Kiyoshi Teshigawara[1], Shiyu Jin[1], Haruhisa Iguchi[4], Ryuji Hiramatsu[4], Derek LeRoith[5], Kiyoshi Takeda[6], Shizuo Akira[6] & Masato Kasuga[1]

The transcription factor, signal transducer and activator of transcription-3 (STAT-3) contributes to various physiological processes. Here we show that mice with liver-specific deficiency in STAT-3, achieved using the Cre-*lox*P system, show insulin resistance associated with increased hepatic expression of gluconeogenic genes. Restoration of hepatic STAT-3 expression in these mice, using adenovirus-mediated gene transfer, corrected the metabolic abnormalities and the alterations in hepatic expression of gluconeogenic genes. Overexpression of STAT-3 in cultured hepatocytes inhibited gluconeogenic gene expression independently of peroxisome proliferator-activated receptor-γ coactivator-1α (PGC-1α), an upstream regulator of gluconeogenic genes. Liver-specific expression of a constitutively active form of STAT-3, achieved by infection with an adenovirus vector, markedly reduced blood glucose, plasma insulin concentrations and hepatic gluconeogenic gene expression in diabetic mice. Hepatic STAT-3 signaling is thus essential for normal glucose homeostasis and may provide new therapeutic targets for diabetes mellitus.

An increase in gluconeogenesis in the liver is largely responsible for the enhanced hepatic glucose production and fasting hyperglycemia in individuals with diabetes mellitus[1]. The regulation of gluconeogenesis is predominantly dependent on the expression of genes that encode enzymes involved in this process, including phosphoenolpyruvate carboxykinase-1 (PCK-1) and glucose 6-phosphatase (G6PC)[2]. The pathophysiological significance of the dysregulation of hepatic gluconeogenic genes is supported not only by increased expression of these genes in models of diabetes[3,4], but also by the glucose intolerance induced by overexpression of *Pck1* or *G6pc* in the liver[5–8].

The expression of these gluconeogenic genes is controlled mainly by insulin and glucagon[9]. Interleukin-6 (IL-6), however, is also implicated in the regulation of these genes. Treatment of hepatocytes with IL-6 reduces the expression of *Pck1* (ref. 10), and transplantation of an IL-6-producing tumor into mice results in inhibition of liver *G6pc* expression[11]. In addition, the serum concentration of IL-6 is increased not only in patients with inflammatory diseases[12], but also in individuals with altered metabolic states, such as those associated with physical training or obesity[13,14]. These observations prompted us to generate mice that lack STAT-3, an important signaling molecule used by the IL-6 family of cytokines[15], specifically in the liver. We now show that liver STAT-3 plays an essential role in normal glucose homeostasis by regulating the expression of gluconeogenic genes. It also provides a new therapeutic target for individuals with diabetes mellitus.

RESULTS

L-ST3KO mice are insulin resistant

We generated mice with liver-specific STAT-3 deficiency using the Cre-*lox*P system. We crossed *Stat3*-heterozygous (*Stat3*$^{+/-}$) knockout mice[16] with Alb-*Cre* mice[17], which express the Cre recombinase gene under the control of the albumin gene promoter, to obtain *Stat3*$^{+/-}$Alb-*Cre* mice. We then bred those mice with mice homozygous for a floxed allele of *Stat3* (*Stat3*$^{flox/flox}$)[18]. We thus obtained animals with the genotypes *Stat3*$^{flox/+}$, *Stat3*$^{flox/-}$, *Stat3*$^{flox/+}$Alb-*Cre* and *Stat3*$^{flox/-}$Alb-*Cre* (L-ST3KO). The presence of *lox*P sequences in *Stat3* did not affect the abundance of the STAT-3 protein[18], and Alb-*Cre* mice did not exhibit metabolic abnormalities[17]. We therefore used *Stat3*$^{flox/+}$, *Stat3*$^{flox/-}$ and L-ST3KO mice for our experiments.

The abundance of STAT-3 in the livers of L-ST3KO mice was <5% of that in the livers of *Stat3*$^{flox/-}$ animals; STAT-3 abundance in other tissues did not differ between the two genotypes (**Fig. 1a**). The body mass of L-ST3KO mice was ~10% greater than that of *Stat3*$^{flox/+}$ and *Stat3*$^{flox/-}$ mice (**Fig. 1b**). Although blood glucose concentrations were similar among mice of all three genotypes (**Fig. 1c**), the plasma insulin concentration of L-ST3KO mice was higher than that of the other two groups of mice at 16 and 24 weeks of age (**Fig. 1d**). Liver mass did not differ between L-ST3KO and *Stat3*$^{flox/-}$ mice (**Supplementary Table 1** online), and the histology of the livers of L-ST3KO mice appeared normal (data not shown). The masses of epi-

[1]Department of Clinical Molecular Medicine, Division of Diabetes and Digestive and Kidney Diseases, Kobe University Graduate School of Medicine, Kobe 650-0017, Japan. [2]Bioengineering Laboratory, Department of Innovative Surgery, National Research Institute for Child Health and Development, Tokyo 154-8567, Japan. [3]Department of Food and Health Science, Okayama University Graduate School of Medicine and Dentistry, Okayama, 700-8558, Japan. [4]Genomics Science Laboratories, Sumitomo Pharmaceuticals Co. Ltd., Takarazuka, Hyogo 665-0051, Japan. [5]Section on Molecular and Cellular Physiology, Diabetes Branch, National Institute of Diabetes and Digestive and Kidney Diseases, National Institutes of Health, Bethesda, Maryland 20892, USA. [6]Department of Host Defense, Research Institute for Microbial Diseases, Osaka University, Osaka 565-0871, Japan. Correspondence should be addressed to M.K. (kasuga@med.kobe-u.ac.jp).

Published online 11 January 2004; doi:10.1038/nm980

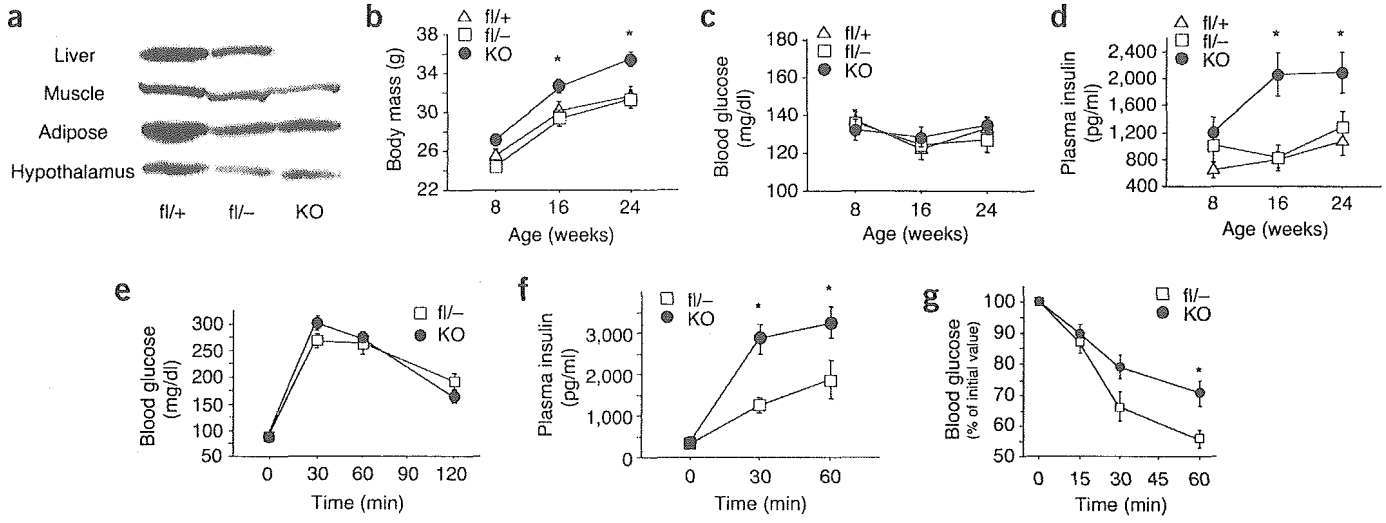

Figure 1 Metabolic phenotypes of mice with liver-specific STAT-3 deficiency (L-ST3KO mice). (**a**) Immunoblot analysis of STAT-3 in total homogenates prepared from indicated organs of *Stat3*$^{flox/+}$ (fl/+), *Stat3*$^{flox/-}$ (fl/–) and L-ST3KO (KO) mice. (**b–d**) Body mass (**b**), blood glucose concentration (**c**) and plasma insulin concentration (**d**) of mice in randomly fed state, at indicated ages. *, $P < 0.05$ by ANOVA, compared with *Stat3*$^{flox/+}$ or *Stat3*$^{flox/-}$ mice. (**e–g**) Blood glucose (**e**) and plasma insulin (**f**) concentrations during intraperitoneal glucose tolerance test, and blood glucose concentration during insulin tolerance test (**g**). *, $P < 0.05$ by Student *t*-test, compared with *Stat3*$^{flox/-}$ mice. Data shown are mean ± s.e.m. of values from 8, 8 and 11 *Stat3*$^{flox/+}$, *Stat3*$^{flox/-}$ and L-ST3KO mice, respectively (**b–d**), and from 9 and 12 *Stat3*$^{flox/-}$ and L-ST3KO mice, respectively (**e–g**), at 22–24 weeks of age.

didymal and inguinal subcutaneous fat in L-ST3KO mice were 2.5× and 1.9×, respectively, that of *Stat3*$^{flox/-}$ mice, but the latter comparison was not statistically significant (Supplementary Table 1 online). Food consumption did not differ between L-ST3KO and *Stat3*$^{flox/-}$ mice. Whereas blood glucose concentrations during a glucose challenge test were similar between L-ST3KO and *Stat3*$^{flox/-}$ mice (Fig. 1e), the increase in plasma insulin concentration during this test was exaggerated in L-ST3KO mice (Fig. 1f). The glucose-lowering effect of exogenously administered insulin was reduced in L-ST3KO mice (Fig. 1g). Euglycemic, hyperinsulinemic clamp analyses revealed that insulin-induced suppression of hepatic glucose output was impaired in L-ST3KO mice, whereas the glucose disposal rate was not significantly altered (Fig. 2a). Consistent with the increased plasma insulin concentration, the size of the pancreatic islets of L-ST3KO mice was increased (Supplementary Table 1 online). When fed a high-fat diet, both plasma insulin and blood glucose concentrations of L-ST3KO mice at 16 and 24 weeks of age were higher than those of *Stat3*$^{flox/-}$ mice (Fig. 2b,c). The responses to glucose and insulin tolerance tests, as well as blood glucose and plasma insulin concentration after high-fat feeding, did not differ between *Stat3*$^{flox/+}$ and *Stat3*$^{flox/-}$ mice (Supplementary Fig. 1 online). These results indicate that L-ST3KO mice are insulin resistant and develop glucose intolerance when fed a high-fat diet, whereas haploinsufficiency of *Stat3* does not affect whole-body insulin sensitivity.

Hepatic gene expression in L-ST3KO mice

Given that STAT-3 is a transcription factor, it was likely that the altered glucose metabolism in L-ST3KO mice was attributable to changes in hepatic gene expression. The abundance of glucokinase,

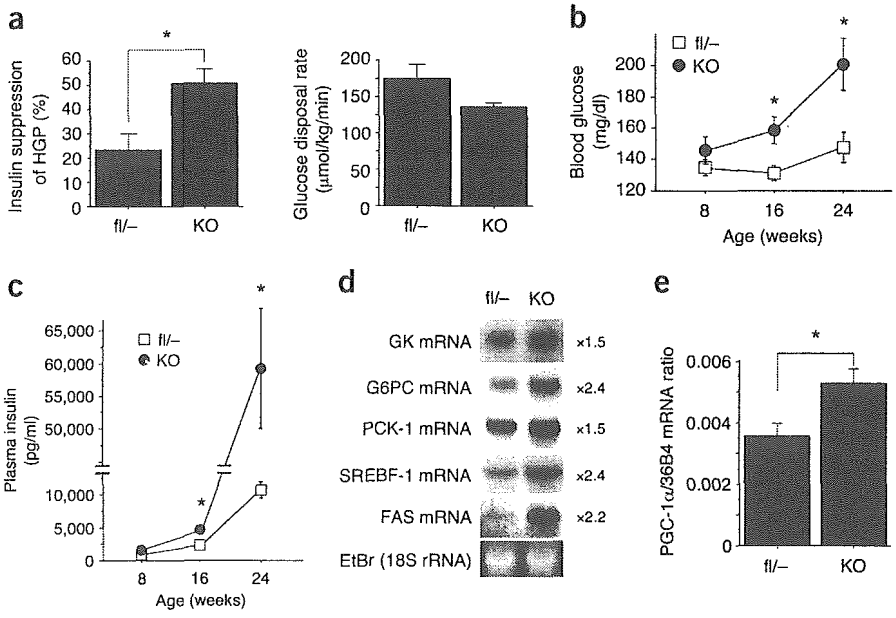

Figure 2 Euglycemic, hyperinsulinemic clamp analyses, effects of high-fat diet and changes in hepatic gene expression in L-ST3KO mice. (**a**) Insulin suppression of hepatic glucose production (left) and glucose disposal rate (right) in 16-week-old *Stat3*$^{flox/-}$ (fl/–) ($n = 4$) or L-ST3KO (KO; $n = 4$) mice, as determined by euglycemic hyperinsulinemic clamp analyses. (**b,c**) Blood glucose (**b**) and plasma insulin (**c**) concentrations in randomly fed state of mice fed high-fat diet or normal chow from 4 to 24 weeks of age. (**d,e**) Northern blot (**d**) and RT-PCR analysis (**e**) of RNA extracted from livers of *Stat3*$^{flox/-}$ ($n = 7$) or L-ST3KO ($n = 8$) mice in randomly fed state at 22–24 weeks of age. GK, glucokinase. Numbers in **d** indicate fold increase in mRNA in L-ST3KO compared with *Stat3*$^{flox/-}$ mice. Ethidium bromide (EtBr) staining of 18S rRNA was used as control. Data in **a–c,e** are mean ± s.e.m. *, $P < 0.05$ by Student *t*-test, compared with corresponding *Stat3*$^{flox/-}$ mice.

G6PC and PCK-1 mRNA was increased ~1.5, 2.4 and 1.5 times, respectively, in the livers of L-ST3KO mice compared with those of *Stat3*$^{flox/-}$ mice (Fig. 2d). In the liver, an increase in the abundance of the transcriptional coactivator PGC-1α induces the expression of *Pck1* and *G6pc* (ref. 19). The abundance of PGC-1α mRNA in the livers of L-ST3KO mice was ~1.5 times that in *Stat3*$^{flox/-}$ mice (Fig. 2e). Sterol regulatory element binding factor-1 (SREBF-1) is a transcription factor that regulates the expression of genes involved in triglyceride synthesis, including the gene encoding fatty acid synthase (*Fasn*)[20]. The expression of *Srebf1* and *Fasn* in the liver increased ~2.4- and 2.2-fold, respectively, in L-ST3KO mice compared with control animals (Fig. 2d). Consistent with the increased expression of these lipogenic genes, the hepatic triglyceride content of L-ST3KO mice was 1.4 times that of *Stat3*$^{flox/-}$ mice (Supplementary Fig. 2 online). Early events of insulin signaling in the liver, including tyrosine phosphorylation of insulin receptor substrates 1 and 2 and phosphorylation of Akt, did not differ between L-ST3KO and *Stat3*$^{flox/-}$ mice after bolus injection of insulin (data not shown).

Restoration of hepatic STAT-3 in L-ST3KO mice

Systemic infusion of adenoviral vectors results in liver-specific expression of exogenous genes[5,21]. Infusion of an adenovirus vector (AxCASTAT-3WT) encoding wild-type STAT-3 resulted in hepatic expression of STAT-3 that was ~2.5 times greater than the apparent STAT-3 expression in *Stat3*$^{flox/-}$ mice infused with a control virus encoding β-galactosidase (Fig. 3a). The restoration of hepatic STAT-3 expression resulted in reduced plasma insulin concentration in L-ST3KO mice fed normal chow or a high-fat diet, and reduced blood glucose concentration in L-ST3KO mice fed a high-fat diet (Fig. 3b–e). This was associated with decreased expression of *Pck1*, *G6pc* and *Ppargc1* (encoding PGC-1α) in the liver (Fig. 3f,g). These results suggest that the changes in glucose metabolism apparent in L-ST3KO mice are attributable to the lack of hepatic STAT-3 signaling.

STAT-3 inhibits expression of gluconeogenic genes

We did *in vitro* experiments to further establish a causal link between STAT-3 deficiency and the changes in hepatic gene expression in L-ST3KO mice. Exposure of cultured rat primary hepatocytes to a nonmetabolizable cyclic AMP analog (8CPT-cAMP) and dexamethasone (Dex/cAMP) resulted in an increase in the expression of *Pck1* and *G6pc*, an effect that was inhibited by the additional presence of insulin (Supplementary Fig. 3 online) or of IL-6 (Fig. 4a). Incubation of the cells with IL-6 induced the tyrosine phosphorylation of STAT-3 (Fig. 4a), which is essential for its activation of target genes[15]. Expression of a dominant-negative mutant of STAT-3 (STAT-3F)[22] by infection with an adenovirus vector prevented the IL-6-induced phosphorylation of STAT-3, as well as the effect of this cytokine on *G6pc* and *Pck1* expression. STAT-3F did not affect insulin-induced suppression of the expression of these genes (Supplementary Fig. 3 online), however, indicating that the IL-6-induced inhibition of *Pck1* and *G6pc* expression is mediated by STAT-3. In addition, expression of wild-type STAT-3 at a level about five times that of the endogenous protein inhibited *Pck1* and *G6pc* expression (Fig. 4b). *Ppargc1* expression in hepatocytes was induced by DEX/cAMP; this effect was inhibited by IL-6 and paralleled the observed changes in the expression of *Pck1* and *G6pc*. The inhibitory effect of IL-6 was blocked by STAT-3F expression and mimicked by overexpression of wild-type STAT-3 (Fig. 4c). In contrast, neither IL-6 treatment nor overexpression of wild-type STAT-3 in hepatocytes affected the basal or insulin-induced expression of *Srebf1*

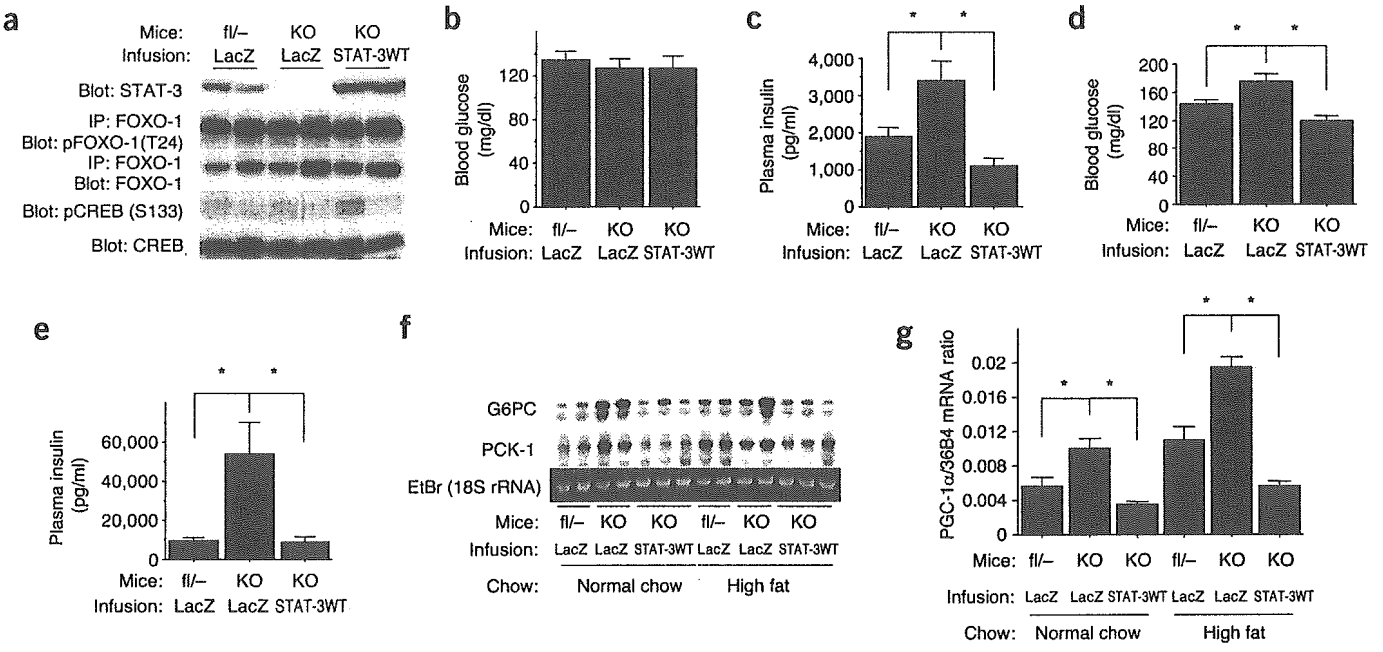

Figure 3 Restoration of STAT-3 expression in livers of L-ST3KO mice. *Stat3*$^{flox/-}$ mice (fl/–) or L-ST3KO (KO) mice (24 weeks old) were fed normal chow (**a–c,f,g**) or high-fat diet (**d–g**). Mice were injected with adenoviruses encoding β-galactosidase (LacZ) or wild-type STAT-3 (STAT-3WT). **a**, Total liver homogenate was subjected to immunoblot analysis using antibodies to STAT-3, CREB or phosphorylated CREB (pCREB), or subjected to immunoprecipitation (IP) using antibodies to FOXO-1 and then to immunoblot analysis using antibodies to FOXO-1 or phosphorylated FOXO-1 (pFOXO-1). Blood glucose (**b,d**) and plasma insulin (**c,e**) concentrations of mice in randomly fed states were also determined. Total RNA was also isolated from liver and subjected to either northern blot analysis with indicated probes (**f**) or to RT-PCR analysis with primers for PGC-1α (**g**). Data in **b–e,g** are mean ± s.e.m. of six mice. *, $P < 0.05$ by ANOVA for the indicated comparisons. Each lane in **a,f** corresponds to an individual mouse.

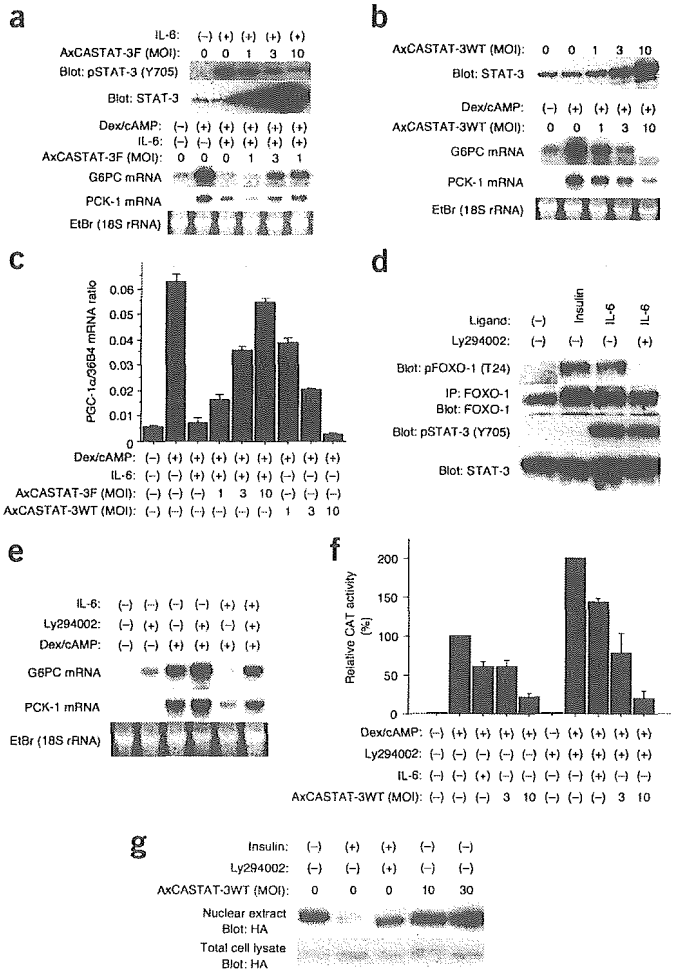

Figure 4 Effects of IL-6, Ly294002 and dominant-negative or wild-type STAT-3 on gluconeogenic genes, FOXO-1 phosphorylation and *Pck1* promoter activity. (**a**,**c**) Primary cultured hepatocytes were infected or not with AxCASTAT-3F vector at indicated multiplicity of infection (MOI; plaque-forming units per cell), and incubated with or without IL-6. Total cell lysates were subjected to immunoblot analysis with antibodies to STAT-3 or tyrosine-phosphorylated STAT-3 (pSTAT-3) (**a**, top two panels). Above experiment was repeated with or without Dex/cAMP (**a**, bottom three panels, and **c**). Total RNA was subjected to either northern blot (**a**, bottom three panels) or RT-PCR analysis (**c**). (**b**) Cells infected or not with AxCASTAT-3WT (encoding wild-type STAT-3) were incubated with or without Dex/cAMP. Total RNA was subjected to either northern blot (**b**, bottom three panels) or RT-PCR analysis (**c**). Total lysates of cells not exposed to Dex/cAMP were also subjected to immunoblot analysis with antibodies to STAT-3 (**b**, top panel). (**d**) Primary cultured hepatocytes were incubated or not with IL-6 or insulin, in the presence or absence of Ly294002. Total cell lysates were subjected to immunoblot analysis with or without prior immunoprecipitation (IP), using antibodies to tyrosine-phosphorylated FOXO-1, tyrosine-phosphorylated STAT-3 or STAT-3. (**e**) Primary cultured hepatocytes were incubated with or without Dex/cAMP, in the absence or presence of IL-6 or Ly294002. Total RNA was subjected to northern blot analysis. (**f**) HL1C cells were infected or not with AxCASTAT3-WT and incubated with or without Dex/cAMP, in the absence or presence of IL-6 or Ly294002. Total cell lysates were subjected to CAT assay. (**g**) Fao cells were infected with adenovirus encoding hemagglutinin (HA)-tagged FOXO-1 and coinfected or not with AxCASTAT-3WT. Cells were then incubated with or without insulin, in the presence or absence of Ly294002. Nuclear extracts or total cell lysates were subjected to immunoblot analysis with antibodies to HA. Northern blot and immunoblot data are representative of three independent experiments; RT-PCR and CAT data are mean ± s.e.m. of values from three experiments.

(**Supplementary Fig. 4** online) or *Gck* (encoding glucokinase; data not shown). These results suggest that STAT-3 signaling does not directly influence the hepatic expression of *Srebf1* and *Gck*, and that the increased expression of these genes in L-ST3KO mice is likely to be caused by secondary metabolic alterations, most probably to plasma insulin concentration.

Phosphoinositide 3-kinase (PI-3K) has a key role in insulin-induced suppression of *Pck1* and *G6pc* expression by inhibiting the transcription factor forkhead box O1 (FOXO-1)[23,24]. In primary cultured hepatocytes, IL-6 and insulin both stimulated phosphorylation of FOXO-1 (**Fig. 4d**), which is important for the translocation of FOXO-1 from the nucleus and inhibition of its transcriptional activity[23,24]. IL-6-induced phosphorylation of FOXO-1 was prevented by Ly294002, an inhibitor of PI-3K. *Pck1* and *G6pc* expression, in hepatocytes exposed to both Dex/cAMP and Ly294002, were greater than in cells exposed to Dex/cAMP alone (**Fig. 4e**), suggesting that basal PI-3K activity contributes to the suppression of *Pck1* and *G6pc* expression. IL-6 inhibited *Pck1* and *G6pc* expression in Ly294002-treated cells, suggesting that IL-6 suppresses the expression of these genes, at least in part through a PI-3K-independent pathway. HL1C cells, which are cultured hepatocytes stably expressing the *Pck1* promoter sequence ligated to the chloramphenicol acetyl transferase (CAT) reporter gene, are widely used to study the transcriptional regulation of *Pck1* (refs. 25,26). Exposure of HL1C cells to Dex/cAMP stimulated CAT activity, which was inhibited by the addition of IL-6 or by overexpression of wild-type STAT-3 (**Fig. 4f**). Ly294002 augmented Dex/cAMP-induced CAT activity, whereas exposure of the cells to IL-6 or overexpression of wild-type STAT-3 inhibited Dex/cAMP-induced CAT activity in the presence of Ly294002. Overexpression of wild-type STAT-3 did not affect the abundance of FOXO-1 protein in the nuclear fraction, which was monitored by exogenously expressed, hemagglutinin-tagged FOXO-1 in Fao rat hepatoma-derived cultured cells, whereas insulin reduced the nuclear abundance of FOXO-1 in a PI-3K-dependent manner (**Fig. 4g**). These results collectively suggest that STAT-3 inhibits *Pck1* and *G6pc* expression via a PI-3K/FOXO-1-independent pathway whereas the effect of IL-6 may be mediated, at least in part, by PI-3K. This hypothesis is consistent with findings that neither STAT-3 deficiency in the liver nor restoration of hepatic STAT-3 in L-ST3KO mice affected the phosphorylation of FOXO-1 in the liver (**Fig. 3a**).

The transcription factor cAMP response element binding protein (CREB) contributes to the expression of *Pck1* and *G6pc*[27]. The phosphorylation of hepatic CREB in *Stat3*$^{flox/-}$ mice infused with a control virus was similar to that observed in L-ST3KO mice infused with a control virus or AxCASTAT-3WT (**Fig. 3a**). Moreover, overexpression of STAT-3 in primary cultured hepatocytes did not affect cAMP-induced phosphorylation of CREB (data not shown), indicating that STAT-3 inhibits *Pck1* and *G6pc* expression thorough a mechanism that is independent of CREB phosphorylation.

STAT-3 suppression of gluconeogenesis is PGC-1α-independent

Given that STAT-3 inhibits the expression of *Pck1* and *G6pc*, as well as their upstream regulator PGC-1α, we investigated whether the effects of STAT-3 on *Pck1* and *G6pc* expression are mediated through the reduction of PGC-1α expression. Treatment of Fao cells (which do not express PGC-1α[24]) with DEX/cAMP induced the expression of *Pck1*. This effect was prevented by overexpression of wild-type STAT-3 (**Fig. 5a**), indicating that STAT-3 inhibits the

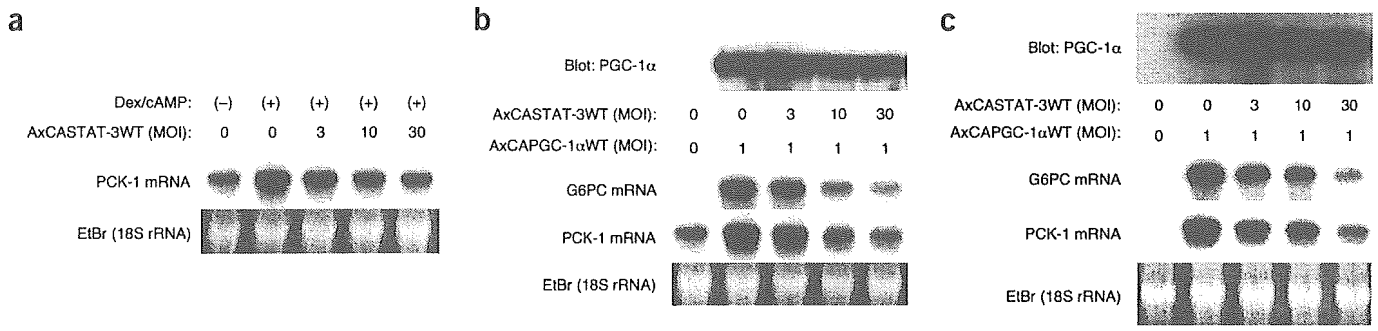

Figure 5 Effects of wild-type STAT-3 on PGC-1α-induced expression of PCK-1 and G6PC. (**a**) Fao cells were infected or not with AxCASTAT3-WT (encoding wild-type STAT-3) and incubated with or without Dex/cAMP. Total RNA was extracted from cells and subjected to northern blot analysis. (**b**,**c**) Fao cells (**b**) or primary cultured hepatocytes (**c**) were infected or not with AxCAPGC-1αWT (encoding wild-type PGC-1α) and coinfected or not with AxCASTAT-3WT. Total cell lysates were subjected to immunoblot analysis with antibodies to PGC-1α (top), and total RNA was subjected to northern blot analysis (bottom). Data shown are representative of three experiments.

expression of *Pck1* in the absence of PGC-1α. Infection of Fao cells with an adenovirus vector encoding PGC-1α increased *Pck1* and *G6pc* expression (Fig. 5b), consistent with a previous report[19]. Coinfection of the cells with AxCASTAT-3WT inhibited PGC-1α-induced expression of *Pck1* and *G6pc* without affecting the abundance of PGC-1α protein. Similar dominant-inhibitory effects of STAT-3 on PGC-1α-induced expression of *Pck1* and *G6pc* were observed in primary cultured hepatocytes (Fig. 5c). These results indicate that STAT-3 is capable of suppressing *Pck1* and *G6pc* expression in a PGC-1α -independent manner.

STAT-3 ameliorates glucose intolerance in diabetic mice

Several animal models of insulin resistance or diabetes exhibit increased expression of *Pck1* and *G6pc* in the liver[3,4]. Given that our data indicate that STAT-3 signaling inhibits the expression of these genes, we attempted to reduce their expression and, consequently, to ameliorate glucose intolerance in diabetic animals by activating STAT-3 signaling in the liver. *Pck1*, *G6pc*, and *Ppargc1* expression was greater in the liver of $Lepr^{-/-}$ diabetic mice—which lack functional leptin receptors[28], are obese and exhibit insulin resistance and diabetes—than in the liver of control ($Lepr^{+/-}$) mice (Fig. 6b,c). Infusion

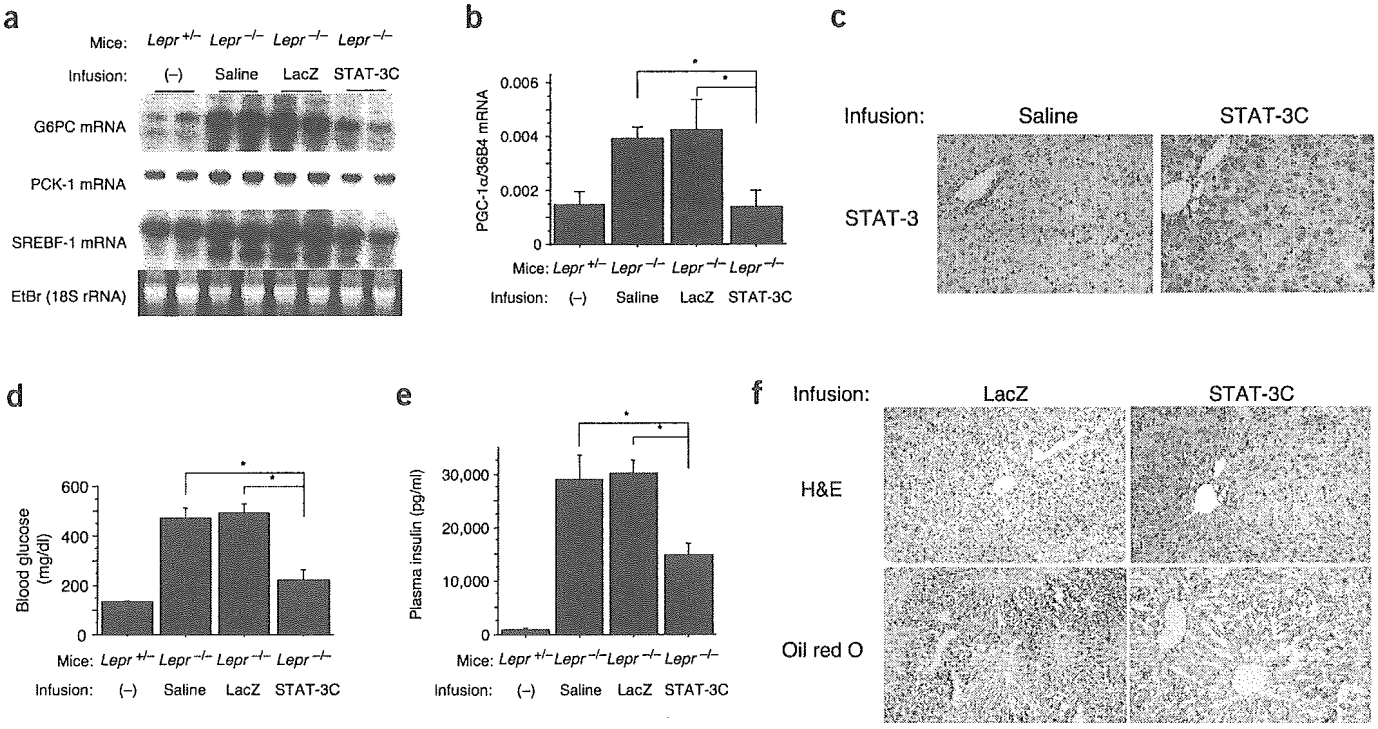

Figure 6 Effects of constitutively active STAT-3 (STAT-3C) on glucose intolerance, gene expression and lipid content in livers of $Lepr^{-/-}$ mice. (**a**,**b**) Northern blot (**a**) and RT-PCR analysis (**b**) of RNA extracted from livers of $Lepr^{+/-}$ and $Lepr^{-/-}$ mice injected with saline or adenovirus vectors encoding β-galactosidase (LacZ) or STAT-3C. (**c**) Immunohistochemical analysis of STAT-3C in livers of $Lepr^{-/-}$ mice injected with saline or STAT-3C-encoding adenovirus. (**d**,**e**) Blood glusoce (**d**) and plasma insulin (**e**) concentrations in $Lepr^{+/-}$ mice and $Lepr^{-/-}$ mice injected with saline, adenovirus vectors encoding β-galactosidase or STAT-3C. (**f**) Histological analysis (H&E or oil red O staining) of livers of $Lepr^{-/-}$ mice injected with adenovirus vectors encoding β-galactosidase or STAT-3-C. Data in **c**,**f** are representative of results obtained from four mice; data in **b**,**d**,**e** are mean ± s.e.m. of results obtained from four mice in randomly fed state. *, $P < 0.05$ by ANOVA (**b**,**d**,**e**).

of an adenovirus vector (AxCASTAT-3C) encoding a FLAG epitope–tagged, constitutively active form of STAT-3 (STAT-3C)[29] into *Lepr*$^{-/-}$ mice resulted in expression of the mutant protein in the liver, but not in skeletal muscle or adipose tissue (data not shown). In the livers of *Lepr*$^{-/-}$ mice infused with saline, endogenous STAT-3 protein was hardly detectable by immunohistochemistry, whereas more than 60% of hepatocytes of *Lepr*$^{-/-}$ mice infused with AxCASTAT3-C were positive for antibodies to STAT-3, indicating efficient gene transfer (**Fig. 6a**). *Pck1*, *G6pc*, and *Pgpargc1* expression in the liver was reduced in *Lepr*$^{-/-}$ mice infused with AxCASTAT3-C, compared with the expression in mice infused with saline or a control virus encoding β-galactosidase (**Fig. 6b,c**). Blood glucose and plasma insulin concentrations in *Lepr*$^{-/-}$ mice were markedly reduced by infusion of AxCASTAT3-C (**Fig. 6d,e**). Expression of STAT-3C in the livers of *Lepr*$^{-/-}$ mice also reduced the steatosis (**Fig. 6f**) and *Srebf1* expression (**Fig. 6b**) apparent in the livers of *Lepr*$^{-/-}$ mice.

DISCUSSION

We have shown that mice lacking STAT-3 specifically in the liver (L-ST3KO mice) exhibit insulin resistance and, when fed a high-fat diet, glucose intolerance. Restoration of hepatic STAT-3 expression in L-ST3KO mice corrected the metabolic abnormalities of these animals. Activation of STAT-3 signaling by expression of a constitutively active form of STAT-3 in the liver also greatly ameliorated glucose intolerance and insulin resistance in *Lepr*$^{-/-}$ diabetic mice. These observations reveal the physiological importance of hepatic STAT-3 signaling in normal glucose homeostasis, and suggest that such signaling is a potential therapeutic target for the treatment of diabetes mellitus.

Pck1 and *G6pc* expression was increased in the liver of L-ST3KO mice, a phenotype that was reversed by exogenously expressed liver STAT-3. Conversely, expression of STAT-3C reduced the expression of these genes in the liver of *Lepr*$^{-/-}$ mice. Together with our confirmatory results obtained with cultured hepatocytes, these observations reveal an inhibitory role for STAT-3 signaling in the expression of *Pck1* and *G6pc*. Given that hepatic glucose production is largely dependent on the expression of gluconeogenic genes[2], and that overexpression of *G6pc* (ref. 5) or *Pck1* (ref. 8) in the liver by a factor of only 2 to 3 results in glucose intolerance, the observed changes in the expression of these genes in the liver is likely to be primarily responsible for the insulin resistance of L-ST3KO mice and for the amelioration of glucose intolerance in *Lepr*$^{-/-}$ mice after STAT3-C expression. Changes in the abundance of PGC-1α mRNA essentially paralleled those of the gluconeogenic gene transcripts in our in *vitro* and *in vivo* experiments. STAT-3, however, can inhibit the expression of *Pck1* and *G6pc* in a PGC-1α-independent manner. It is therefore possible that STAT-3 reduces the expression of *Pck1* and *G6pc* through both PGC-1α-dependent and PGC-1α-independent pathways. The PI-3K/FOXO-1 pathway also has an important role in insulin-induced suppression of *Pck1* and *G6pc* expression[23,24]. STAT-3 inhibited the expression of *Pck1* and *G6pc* in the presence of an inhibitor of PI-3K. In addition, STAT-3 did not affect the nuclear abundance of FOXO-1, suggesting that the inhibitory effects of STAT-3 on *Pck1* and *G6pc* expression do not depend on the PI-3K/FOXO-1 pathway.

Hypoglycemia in mice injected with lipopolysaccharide, a model of endotoxic shock, was prevented by the administration of neutralizing antibodies to IL-6 (ref. 30), suggesting that IL-6 induces hypoglycemia during severe infection, probably through the mechanism uncovered in the present study. The serum concentration of IL-6 is increased not only in infectious and inflammatory disease, but also during various physiopathological conditions such as physical training and obesity[12–14]. The IL-6–STAT-3 signaling pathway in the liver may thus contribute to carbohydrate metabolism during such conditions. However, the development of insulin resistance in L-ST3KO mice indicates that hepatic STAT-3 is important in glucose homeostasis not only in pathological conditions, but also under normal physiological conditions. The identity of the ligands responsible for the STAT-3-dependent regulation of hepatic gluconeogenesis under physiological conditions remains to be determined. Although disruption of the IL-6-encoding gene in mice results in insulin resistance and obesity, this phenotype is likely to be attributable to the lack of IL-6 action in the central nervous system[31]; the peripheral effects of this cytokine on glucose metabolism are unclear. We have observed a low level of STAT-3 phosphorylation in the livers of mice under normal physiological conditions (H. Inoue *et al.*, unpublished data), suggesting that continuous, low-level activation of STAT-3 signaling may be necessary to maintain basal expression of gluconeogenic genes.

Insulin stimulates the uptake of glucose into adipocytes and the subsequent synthesis of triglyceride from the hexose[32]. Insulin resistance restricted to the liver might thus increase hepatic glucose output and, concomitantly, promote glucose uptake and triglyceride synthesis in adipocytes as a result of the associated hyperinsulinemia. Such a shift in energy sources may account for the increased adiposity in L-ST3KO mice. Transgenic rats that overexpress *Pck1* in the liver and kidneys exhibit increased body mass and hyperinsulinemia[7].

We have shown by loss-of-function and gain-of-function experiments that STAT-3 signaling has a crucial role in the expression of gluconeogenic genes in the liver, as well as in normal glucose homeostasis *in vivo*. The STAT-3 signaling pathway responsible for the regulation of gluconeogenesis in the liver may thus provide new therapeutic targets for the treatment of diabetes mellitus.

METHODS

Mice and adenovirus vectors. Mouse experiments were performed according to the guidelines of the animal ethics committee of Kobe University Graduate School of Medicine. *Stat3*$^{flox/flox}$, *Stat3*$^{-/-}$, and Alb-*Cre* mice were generated as described[16–18]. Only male mice were used for experiments. In experiments examining the effects of a high-fat diet, mice were fed, from 4 to 24 weeks of age, chow containing 30% fat by weight (14% bovine fat, 14% porcine fat and 2% soybean oil). We used PCR to synthesize cDNA encoding mouse PGC-1α. cDNAs encoding wild-type STAT-3 and dominant-negative STAT-3 (STAT-3F), in which Tyr705 is replaced by phenylalanine, were as described[22]. The cDNA encoding a FLAG epitope–tagged, constitutively active form of STAT-3 (STAT-3C)[29], in which Ala662 and Asn664 are replaced with cysteine, was provided by J.E. Darnell Jr. (The Rockefeller University). Adenovirus vectors containing these cDNAs were generated as described[33]. A control virus encoding β-galactosidase was constructed as described[34]. An adenovirus encoding a hemagglutinin epitope–tagged, wild-type FOXO-1 (ref. 23) was provided by D. Accili (Columbia University).

Physiological analyses. Intraperitoneal glucose tolerance and insulin tolerance tests were done as described[21]. Euglycemic hyperinsulinemic clamp studies were done using fasted, conscious mice, essentially as described[35] with the following modifications. [3-^{3}H]glucose was infused throughout the clamp study to determine glucose turnover rate. After a bolus injection (10 μCi), [3-^{3}H]glucose was continuously infused at a rate of 0.1 μCi/min for 2 h. For the measurement of basal glucose turnover rate, blood samples were collected 120 min after the initiation of [3-^{3}H]glucose infusion. Insulin was infused at a rate of 2.5 mU/kg for 120 min, while 40% glucose was infused by variable infusion pump. Blood samples from tail-tip bleeds were collected every 10 min for glucose estimation. Plasma glucose was clamped at 100–120 mg/dl. While glucose levels remained steady, three blood samples were taken for determination of [3-^{3}H]glucose-specific activity. Analysis of [3-^{3}H]glucose measurements and calculation of glucose disposal rates and hepatic glucose production rates were done as described[35].

Northern blot, real-time quantitative RT-PCR and hepatocyte cultures. Total RNA (~15 μg) extracted from organs or cells was subjected to northern blot analysis with probes[21,36] essentially as described[37]. Autoradiograms were visualized and signal intensity was quantitated with a BAS2000 image analyzer (Fujifilm). Primary cultures of rat hepatocytes were prepared and subjected to adenovirus infection as described[37]. HL1C cells, which contain a *Pck1* promoter sequence fused to the CAT reporter gene, were provided by D.K. Granner (Vanderbilt University). For STAT-3 and FOXO-1 phosphorylation experiments, cells were incubated with either IL-6 (50 ng/ml), insulin (100 nM) or Ly294002 (30 μM) for 10 min, and total cell lysates were subjected to immunoblot analysis with antibodies to STAT-3 (Santa Cruz Biotechnology), tyrosine-phosphorylated STAT-3 (Cell Signaling) or tyrosine-phosphorylated FOXO-1 (Cell Signaling). Antibodies to FOXO-1 for immunoprecipitation and immunoblot analysis were obtained from Upstate Biotechnology and Santa Cruz Biotechnology, respectively. CREB phosphorylation was evaluated by immunoblot analysis using antibodies to the phosphorylated forms of CREB (Cell Signaling). For gene expression experiments, cells infected or not with adenoviruses were incubated for 6 h with 500 nM dexamethasone and 0.1 mM 8CPT-cAMP, in the absence or presence of IL-6 (50 ng/ml), insulin (100 nM) or Ly294002 (30 μM). Real-time quantitative RT-PCR analysis was done with a Sequence Detector (model 7900, Applied Biosystems) using 36B4 mRNA as the invariant control, as described[21,36]. The primers used were as follows: mouse PGC-1α, 5′-ATACCGCAAAGAG-CACGAGAAG-3′ (sense) and 5′-CTCAAGAGCAGCGAAAGCGTCACAG-3′ (antisense); rat PGC-1α, 5′- ATGGTTTCATTACCTACCGTTACAC-3′ (sense) and 5′-AAGCAGGGTCAAAATCGTCTGAGT-3′ (antisense); and rat 36B4, 5′-GACAATGGCAGCATCTAC-3′ (sense) and 5′-CAACAGTCGGGGT-3′ (antisense). The primers for mouse 36B4 were as described previously[21].

Adenovirus-mediated gene transduction. L-ST3KO mice and *Stat3*$^{flox/-}$ mice were fed normal or high-fat chow from 4 to 24 weeks of age. Mice were then injected through the tail vein with adenoviral vectors encoding either STAT-3 or β-galactosidase, at a dose of 1×10^8 plaque-forming units. Male *Lepr*$^{-/-}$ mice (C57BL/KsJ-db/db) and control *Lepr*$^{+/-}$ mice (C57BL/KsJ-db/+m; 8–9 weeks of age; Clea Japan) were injected through the tail vein with adenoviral vectors encoding either STAT3-C or β-galactosidase, at a dose of 3×10^8 plaque-forming units. Experiments were done 7 d after adenovirus injection.

Note: Supplementary information is available on the Nature Medicine website.

ACKNOWLEDGMENTS

We thank J.E. Darnell Jr. for the STAT-3C-encoding cDNA, T. Noguchi for the *Gck* probe, H. Shimano for the *Srebf1* probe, H. Nakajima for the *G6pc* probe, N. Iritani for the *Fasn* probe, D. Accili for the adenovirus encoding hemagglutinin-tagged, wild-type FOXO-1, and D.K. Granner for the HL1C cells. This work was supported by a grant from the Ministry of Education, Culture, Sports, Science, and Technology of Japan (to M.K. and W.O.) and a grant from the Cooperative Link of Unique Science and Technology for Economy Revitalization (to M.K.).

COMPETING INTERESTS STATEMENT

The authors declare that they have no competing financial interests.

Received 8 October; accepted 9 December 2003
Published online at http://www.nature.com/naturemedicine/

1. Taylor, S. I. Deconstructing type 2 diabetes. *Cell* **97**, 9–12 (1999).
2. Radziuk, J. & Pye, S. Hepatic glucose uptake, gluconeogenesis and the regulation of glycogen synthesis. *Diabet. Metab. Res. Rev.* **17**, 250–272 (2001).
3. Shimomura, I. *et al.* Decreased IRS-2 and increased SREBP-1c lead to mixed insulin resistance and sensitivity in livers of lipodystrophic and ob/ob mice. *Mol. Cell* **6**, 77–86 (2000).
4. Michael, M.D. *et al.* Loss of insulin signaling in hepatocytes leads to severe insulin resistance and progressive hepatic dysfunction. *Mol. Cell* **6**, 87–97 (2000).
5. Trinh, K.Y., O'Doherty, R.M., Anderson, P., Lange, A.J. & Newgard, C.B. Perturbation of fuel homeostasis caused by overexpression of the glucose-6-phosphatase catalytic subunit in liver of normal rats. *J. Biol. Chem.* **273**, 31615–31620 (1998).
6. Valera, A., Pujol, A., Pelegrin, M. & Bosch, F. Transgenic mice overexpressing phosphoenolpyruvate carboxykinase develop non-insulin-dependent diabetes mellitus. *Proc. Natl. Acad. Sci. USA* **91**, 9151–9154 (1994).
7. Rosella, G. *et al.* Impaired glucose tolerance and increased weight gain in transgenic rats overexpressing a non-insulin-responsive phosphoenolpyruvate carboxykinase gene. *Mol. Endocrinol.* **9**, 1396–1404 (1995).
8. Sun, Y. *et al.* Phosphoenolpyruvate carboxykinase overexpression selectively attenuates insulin signaling and hepatic insulin sensitivity in transgenic mice. *J. Biol. Chem.* **277**, 23301–23307 (2002).
9. O'Brien, R.M. & Granner, D.K. Regulation of gene expression by insulin. *Physiol. Rev.* **76**, 1109–1161 (1996).
10. Christ, B., Yazici, E. & Nath, A. Phosphatidylinositol 3-kinase and protein kinase C contribute to the inhibition by interleukin 6 of phosphoenolpyruvate carboxykinase gene expression in cultured rat hepatocytes. *Hepatology* **31**,461–468 (2000).
11. Metzger, S. *et al.* Interleukin-6 secretion in mice is associated with reduced glucose-6-phosphatase and liver glycogen levels. *Am. J. Physiol.* **273**, E262–E267 (1997).
12. Akira, S., Taga, T. & Kishimoto, T. Interleukin-6 in biology and medicine. *Adv. Immunol.* **54**, 1–78 (1993).
13. Febbraio, M.A. & Pedersen, B.K. Muscle-derived interleukin-6: mechanisms for activation and possible biological roles. *FASEB J.* **16**, 1335–1347 (2002).
14. Vgontzas, A.N., Papanicolaou, D.A., Bixler, E.O., Kales, A., Tyson, K., & Chrousos, G.P. Elevation of plasma cytokines in disorders of excessive daytime sleepiness: role of sleep disturbance and obesity. *J. Clin. Endocrinol. Metab.* **82**,1313-1316 (1997).
15. Levy, D.E. & Lee, C.-K. What does Stat3 do? *J. Clin. Invest.* **109**, 1143–1148 (2002).
16. Takeda, K. *et al.* Targeted disruption of the mouse Stat3 gene leads to early embryonic lethality. *Proc. Natl. Acad. Sci. USA* **94**, 3801–3804 (1997).
17. Yaker, S. *et al.* Normal growth and development in the absence of hepatic insulin-like growth factor I. *Proc. Natl. Acad. Sci. USA* **96**, 7324–7329 (1999).
18. Takeda, K. *et al.* Stat3 activation is responsible for IL-6-dependent T cell proliferation through preventing apoptosis: generation and characterization of T cell-specific Stat3-deficient mice. *J. Immunol.* **161**, 4652–4560 (1998).
19. Yoon, J.C. *et al.* Control of hepatic gluconeogenesis through the transcriptional coactivator PGC-1. *Nature* **413**, 131–138 (2001).
20. Horton, J.D., Goldstein, J.L. & Brown, M.S. SREBPs: activators of the complete program of cholesterol and fatty acid synthesis in the liver. *J. Clin. Invest.* **109**, 1125–1131 (2002).
21. Miyake, K. *et al.* Hyperinsulinemia, glucose intolerance, and dyslipidemia induced by acute inhibition of phosphoinositide 3-kinase signaling in the liver. *J. Clin. Invest.* **110**,1483-1491 (2002).
22. Minami, M. *et al.* STAT3 activation is a critical step in gp130-mediated terminal differentiation and growth arrest of a myeloid cell line. *Proc. Natl. Acad. Sci. USA* **93**, 3963–3966 (1996).
23. Nakae, J., Kitamura, T., Silver, D.L., & Accili, D. The forkhead transcription factor Foxo1 (Fkhr) confers insulin sensitivity. onto glucose-6-phosphatase expression. *J. Clin. Invest.* **108**, 1359-67 (2001).
24. Puigserver, P *et al.* Insulin-regulated hepatic gluconeogenesis through FOXO1-PGC-1a interaction. *Nature* **423**, 550-555. (2003).
25. Scott, D.K., O'Doherty, R.M., Stafford, J.M., Newgard, C.B., & Granner, D.K. Therepression of hormone-activated PEPCK gene expression by glucose is insulin-independent but requires glucose metabolism. *J. Biol. Chem.* 273, 24145-24151 (1998).
26. Kotani, K *et al.* Dominant negative forms of Akt (protein kinase B) and atypical protein kinase Cλ do not prevent insulin inhibition of phosphoenolpyruvate carboxykinase gene transcription. *J. Biol. Chem.* **274**, 21305-21312 (1998).
27. Herzig, S *et al.* CREB regulates hepatic gluconeogenesis through the coactivator PGC-1. *Nature* **413**, 179-183 (2001).
28. Lee, G.-H. *et al.* Abnormal splicing of the leptin receptor in diabetic mice. *Nature* **379**, 632–635 (1996).
29. Bromberg, J.F. *et al.* Stat3 as an oncogene. *Cell* **98**, 295–303 (1999).
30. Strassmann, G., Fong, M., Windsor, S. & Neta, R. The role of interleukin-6 in lipopolysaccharide-induced weight loss, hypoglycemia and fibrinogen production in vivo. *Cytokine* **5**, 285–290 (1993).
31. Wallenius, V. *et al.* Interleukin-6-deficient mice develop mature-onset obesity. *Nature Med.* **8**, 75–79 (2002).
32. Bluher, M *et al.* Adipose tissue selective insulin receptor knockout protects against obesity and obesity-related glucose intolerance. *Dev. Cell.* **3**, 25-38 (2002).
33. Kitamura, T. *et al.* Insulin-induced phosphorylation and activation of cyclic nucleotide phosphodiesterase 3B by the serine-threonine kinase Akt. *Mol. Cell. Biol.* **19**, 6286-6296 (1999).
34. Ozaki, M. *et al.* Inhibition of the Rac1 GTPase protects against nonlethal ischemia/reperfusion-induced necrosis and apoptosis in vivo. *FASEB J.* **14**, 418–429 (2000).
35. Ren, J.M., Marshal,l B.A., Mueckler, M.M., McCaleb, M., Amatruda, J.M., & Shulman, G.I. Overexpression of Glut4 protein in muscle increases basal and insulin-stimulated whole body glucose disposal in conscious mice. *J. Clin. Invest.* **95**, 429-432 (1995).
36. Matsumoto, M. *et al.* PKCλ in liver mediates insulin-induced SREBP-1c expression and determines both hepatic lipid content and overall insulin sensitivity. *J. Clin. Invest.* **112**, 935–944 (2003).
37. Matsumoto, M. *et al.* Role of the insulin receptor substrate 1 and phosphatidylinositol 3-kinase signaling pathway in insulin-induced expression of sterol regulatory element binding protein 1c and glucokinase genes in rat hepatocytes. *Diabetes* **51**, 1672–1680 (2002).

29. Inohara, N. & Nunez, G. NODs: intracellular proteins involved in inflammation and apoptosis. *Nature Rev. Immunol.* **3**, 371–382 (2003).
30. Ruefli-Brasse, A. A., Lee, W. P., Hurst, S. & Dixit, V. M. Rip2 participates in Bcl10 signaling and T-cell receptor-mediated NF-κB activation. *J. Biol. Chem.* **279**, 1570–1574 (2004).

Supplementary Information accompanies the paper on **www.nature.com/nature**.

Acknowledgements We thank D. Dornan and other members of the Dixit laboratory for discussions, E. Humke for help with illustrations, and K. O'Rourke, D. Wadley, Z. Gu, C. Olsson, M. Bauer, L. Tom, J. Kloss, M. Fuentes, M. Osborn, C. Tan, J. Hongo, T. Wong and A. Chuntharapai for technical assistance.

Competing interests statement The authors declare that they have no competing financial interests.

Correspondence and requests for materials should be addressed to V.M.D. (dixit@gene.com).

Regulation of Toll/IL-1-receptor-mediated gene expression by the inducible nuclear protein IκBζ

Masahiro Yamamoto[1], Soh Yamazaki[3], Satoshi Uematsu[1], Shintaro Sato[1,2], Hiroaki Hemmi[1], Katsuaki Hoshino[6], Tsuneyasu Kaisho[6], Hirotaka Kuwata[1], Osamu Takeuchi[1,2], Koichiro Takeshige[3], Tatsuya Saitoh[7], Shoji Yamaoka[7], Naoki Yamamoto[7], Shunsuke Yamamoto[8], Tatsushi Muta[3,4], Kiyoshi Takeda[5] & Shizuo Akira[1,2]

[1]*Department of Host Defense, Research Institute for Microbial Diseases, Osaka University,* [2]*ERATO, Japan Science and Technology Agency, 3-1 Yamada-oka, Suita Osaka 565-0871, Japan*
[3]*Department of Molecular and Cellular Biochemistry, Graduate School of Medical Sciences,* [4]*PRESTO, Japan Science and Technology Agency,* [5]*Department of Embryonic and Genetic Engineering, Medical Institute of Bioregulation, Kyushu University, 3-1-1 Maidashi, Higashi-ku, Fukuoka 812-8582, Japan*
[6]*RIKEN Research Center for Allergy and Immunology, 1-7-22 Suehiro-cho, Tsurumi-ku, Yokohama, Kanagawa 230-0045, Japan*
[7]*Department of Molecular Virology, Graduate School of Medicine, Tokyo Medical and Dental University, 1-5-45 Yushima, Bunkyo-ku, Tokyo 113-8519, Japan*
[8]*Department of Food and Nutrition, Beppu University, Kita-ishigaki, Beppu, Oita 874-0851, Japan*

Toll-like receptors (TLRs) recognize microbial components and trigger the inflammatory and immune responses against pathogens. IκBζ (also known as MAIL and INAP) is an ankyrin-repeat-containing nuclear protein that is highly homologous to the IκB family member Bcl-3 (refs 1–6). Transcription of IκBζ is rapidly induced by stimulation with TLR ligands and interleukin-1 (IL-1). Here we show that IκBζ is indispensable for the expression of a subset of genes activated in TLR/IL-1R signalling pathways. IκBζ-deficient cells show severe impairment of IL-6 production in response to a variety of TLR ligands as well as IL-1, but not in response to tumour-necrosis factor-α. Endogenous IκBζ specifically associates with the p50 subunit of NF-κB, and is recruited to the NF-κB binding site of the IL-6 promoter on stimulation. Moreover, NF-κB1/p50-deficient mice show responses to TLR/IL-1R ligands similar to those of IκBζ-deficient mice. Endotoxin-induced expression of other genes such as *Il12b* and *Csf2* is also abrogated in IκBζ-deficient macrophages. Given that the lipopolysaccharide-induced transcription of IκBζ occurs earlier than transcription of these genes, some TLR/IL-1R-mediated responses may be regulated in a gene expression process of at least two steps that requires inducible IκBζ.

IκBζ is thought to be induced in response to IL-1 or lipopolysaccharide (LPS) (TLR4 ligand)[4–6]. In addition to IL-1 and LPS, IκBζ messenger RNA was strongly upregulated on stimulation with peptidoglycan (PGN) (TLR2 ligand), bacterial lipoprotein (BLP) (TLR1/TLR2), flagellin (TLR5), MALP-2 (TLR6/TLR2), R-848 (TLR7) and CpG DNA (TLR9), but not with tumour-necrosis factor-α (TNF-α) (Fig. 1a). In contrast, other IκB family members such as IκBα and Bcl-3 were induced in response to TNF-α as well as the TLR ligands and IL-1. Thus, IκBζ is induced in the TLR/IL-1R signalling pathway but not the TNF signalling pathway. Furthermore, IL-1- or LPS-induced expression of IκBζ was completely abolished in *MyD88*$^{-/-}$ embryonic fibroblasts (MEFs; Fig. 1b), showing that IκBζ is inducible in the MyD88-dependent part of the TLR/IL-1R signalling pathway[7–15].

To elucidate the physiological role of IκBζ in the TLR/IL-1R response, we generated *IκBζ*$^{-/-}$ mice by targeted gene disruption (see Supplementary Discussion 1 and Supplementary Fig. 1a–d). *IκBζ*$^{-/-}$ splenocytes showed defective proliferation in response to LPS but not to anti-CD40, IL-4 and anti-IgM (Supplementary Fig. 1e, f), suggesting that the TLR4 response is impaired in *IκBζ*$^{-/-}$ cells. Moreover, although *IκBζ*$^{-/-}$ mice grew normally after birth, some of them started to develop atopic dermatitis-like skin lesions with acanthosis and lichenoid changes at the age of 4–5 weeks (Supplementary Fig. 2a, b). All *IκBζ*$^{-/-}$ mice developed the disease by the age of 10 weeks. Histological analysis of 5-week-old *IκBζ*$^{-/-}$ mice showed pathological changes in the conjunctiva, including a heavy lymphocyte infiltration into the submucosa and loss of goblet cells in the conjunctival epithelium (Supplementary Fig. 2c–f).

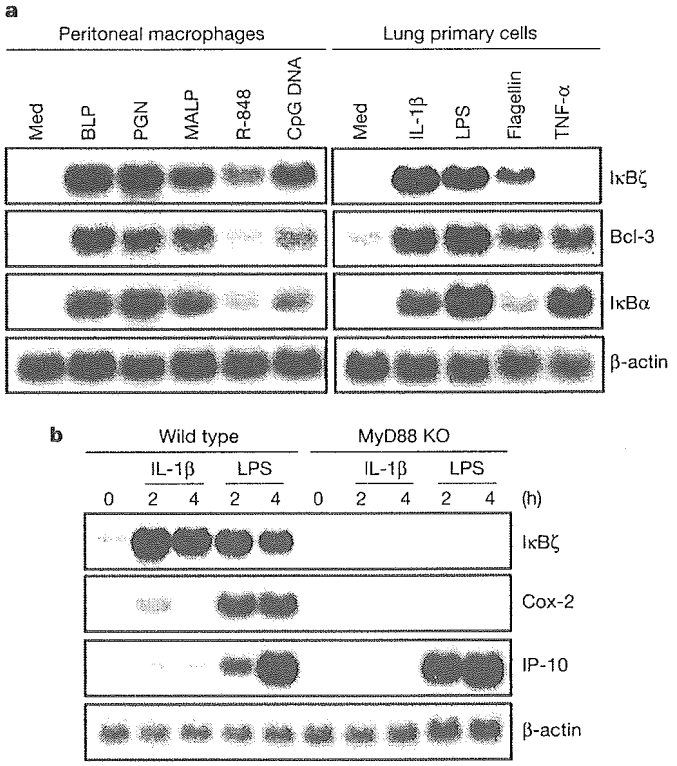

Figure 1 Specific induction of IκBζ on stimulation by TLR/IL-1R ligands. **a**, The indicated cells were stimulated with 100 ng ml^{-1} BLP, 10 μg ml^{-1} PGN, 30 ng ml^{-1} MALP-2, 100 nM R-848, 3 μM CpG DNA, 10 ng ml^{-1} IL-1β, 10 μg ml^{-1} LPS, 100 ng ml^{-1} flagellin and 10 ng ml^{-1} TNF-α for 2 h. Total RNA (10 μg) was extracted and subjected to northern blot analysis for expression of IκBζ, Bcl-3, IκBα and β-actin. Med, medium. **b**, *MyD88*$^{+/+}$ (wild type) and *MyD88*$^{-/-}$ (KO) MEFs were stimulated with 10 ng ml^{-1} IL-1β and 10 μg ml^{-1} LPS for the indicated periods. Total RNA (10 μg) was extracted and subjected to northern blot analysis for expression of IκBζ, Cox-2, IP-10 and β-actin.

We analysed the LPS-induced production of inflammatory mediators in macrophages. *IκBζ*$^{+/+}$ macrophages produced TNF-α, IL-6 and nitric oxide (NO) in response to LPS (Fig. 2a). Although LPS-induced production of TNF-α and NO was normal, production of IL-6 was severely impaired in *IκBζ*$^{-/-}$ macrophages. In addition, production of IL-6 via stimulation by various TLR ligands was also profoundly inhibited in *IκBζ*$^{-/-}$ cells (Fig. 2b–d). Moreover, *IκBζ*$^{-/-}$ cells exhibited defective IL-1-induced IL-6 production; however, IL-1-induced activation of NF-κB and mitogen-activated protein kinases was not impaired in these cells, indicating that there is no defect in the intracellular signalling pathways (Supplementary Fig. 3a, b). On the other hand, TNF-α-induced IL-6 production was not impaired in *IκBζ*$^{-/-}$ cells (Fig. 2e). The impaired production of IL-6 in response to LPS correlated well with the reduced induction of IL-6 mRNA in *IκBζ*$^{-/-}$ cells (Fig. 2f).

When full-length or a deletion mutant form of IκBζ was transfected into MEFs, full-length IκBζ, but not the deletion mutant, rescued the defective production of IL-6 on stimulation with IL-1 in *IκBζ*$^{-/-}$ cells (Fig. 2g), suggesting that expression of IκBζ is required for TLR/IL-1-mediated production of IL-6. As the genes for IκBζ and IL-6 are inducible in response to TLR ligands and IL-1 (refs 4–6, 16, 17), we compared the time course of mRNA expression in macrophages. On stimulation with LPS, induction of IκBζ expression was observed at 30 min and reached maximal levels after 120 min. On the other hand, induction of IL-6 mRNA occurred at later time points compared with IκBζ or TNF-α (Fig. 2h). Taken together, these results indicate that the TLR/IL-1R-mediated expression of the IL-6 gene (*Il6*) requires the preceding induction of IκBζ. Given that IκBζ is also an inducible protein in TLR/IL-1R-mediated signalling pathways, the TLR/IL-1R-mediated production of pro-inflammatory IL-6 may be controlled in at least a two-step fashion.

Our data and those of a previous study[5] indicate the positive role of IκBζ in the TLR/IL-1R-mediated expression of IL-6. To test

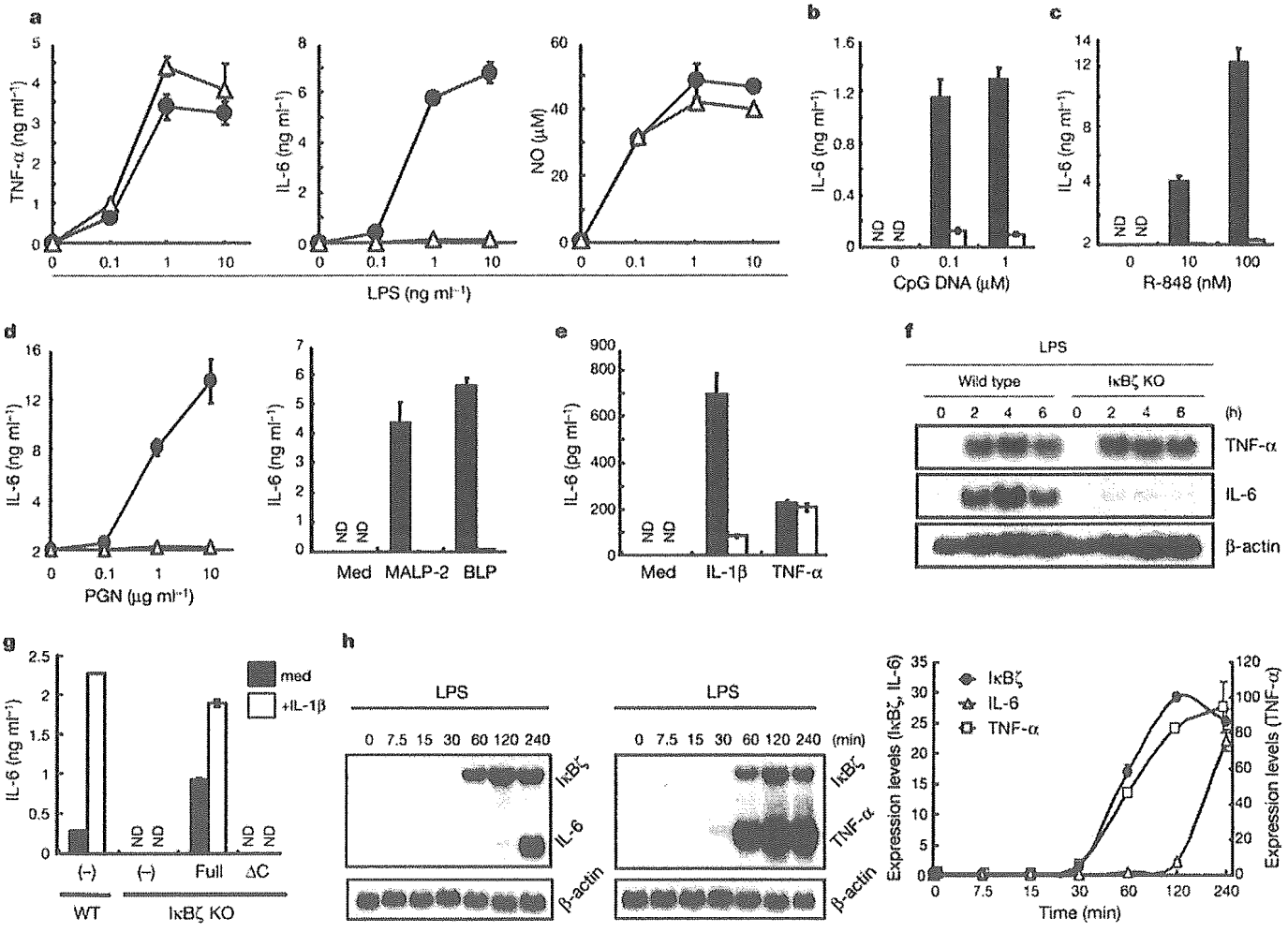

Figure 2 Immune responses in *IκBζ*$^{-/-}$ cells and kinetics of IκBζ induction. **a–d**, *IκBζ*$^{+/+}$ (filled symbols/columns) and *IκBζ*$^{-/-}$ (open symbols/columns) peritoneal macrophages were cultured with 10 ng ml^{-1} LPS, 100 ng ml^{-1} BLP, 30 ng ml^{-1} MALP-2, and the indicated concentrations of PGN, R-848 and CpG DNA in the presence of 30 ng ml^{-1} IFN-γ for 24 h. Values are means ± s.d. of triplicate experiments. ND, not detected. **e**, *IκBζ*$^{+/+}$ (filled columns) and *IκBζ*$^{-/-}$ (open columns) MEFs were stimulated with 10 ng ml^{-1} IL-1β and 10 ng ml^{-1} TNF-α. Values are means ± s.d. of triplicate experiments. **f**, Peritoneal macrophages were stimulated with 10 ng ml^{-1} LPS for the indicated periods. Total RNA (5 μg) was extracted and subjected to northern blot analysis for expression of IL-6, TNF-α and β-actin. **g**, Rescue of IL-1 responsiveness in *IκBζ*$^{-/-}$ MEFs by retroviral transfection with full-length (Full), but not deletion mutant (ΔC), IκBζ. Indicated values are means ± s.d. of triplicate experiments. **h**, Double RNA products indicative of IκBζ, IL-6 and TNF-α mRNA transcripts after LPS simulation of wild-type peritoneal macrophages resolved by electrophoresis. Two independent experiments with independently derived wild-type cells were quantified by Phospholmager (left and middle panels), and mRNA abundance (right panel) is shown for the indicated genes in arbitrary units (left axis, IκBζ and IL-6; right axis, TNF-α) relative to β-actin. Indicated values are means ± s.d. of duplicate experiments.

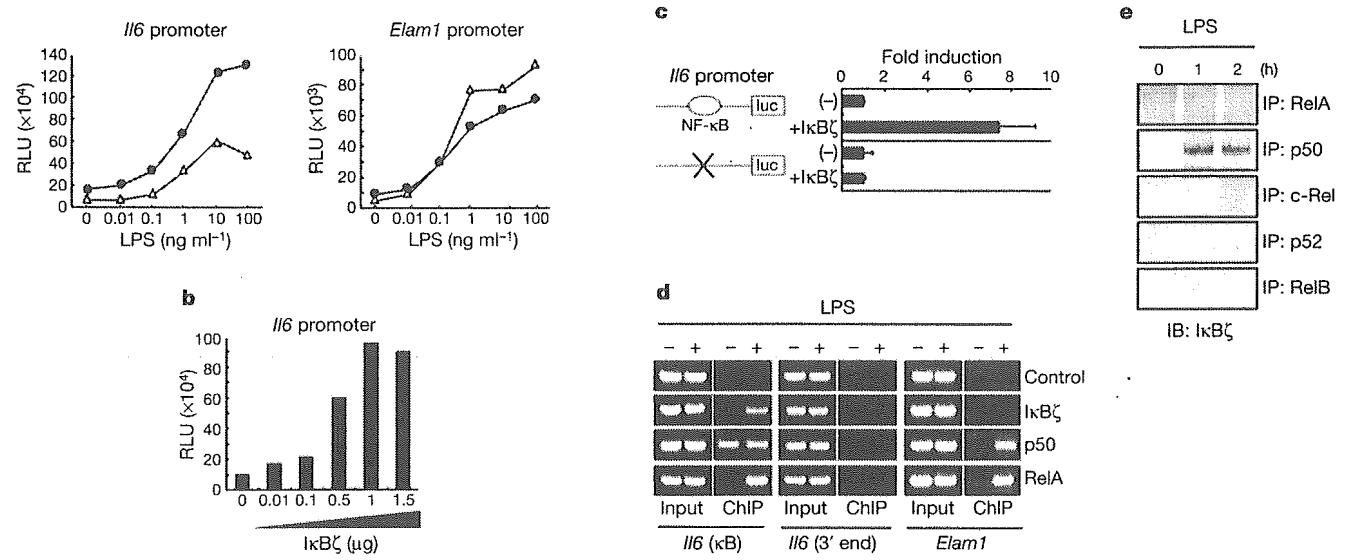

Figure 3 *In vitro* analysis of IκBζ on the *Il6* promoter. **a**, RAW 264.7 cells were transiently transfected with luciferase reporter constructs of either the murine *Il6* promoter or the *Elam1* promoter together with either control (open symbols) or the IκBζ expression plasmid (filled symbols). Luciferase activities are expressed as fold-increase values over the background shown by lysates prepared from untransfected cells. Data are representative of three separate experiments. Cells were stimulated with the indicated concentrations of LPS. RLU, relative luciferase units. **b**, Untreated RAW 264.7 cells were transiently transfected with the IκBζ expression vector together with constant amounts of the *Il6* reporter plasmid. Data are representative of three separate experiments. **c**, P19 cells were transiently transfected with either wild-type or mutant *Il6* promoter reporter constructs together with either control or the IκBζ expression plasmid. Luciferase activities were normalized in each case by dividing the fold-increase values of IκBζ-expressed cells over the background values of lysates with that of mock-expressed cells. Values are means ± s.d. of triplicate experiments. **d**, Chromatin from untreated (−) or LPS-treated (+) (1 μg ml^{-1} for 3 h) RAW 264.7 cells was used for ChIP assays with the indicated antibodies. Precipitated DNA for the *Il6* κB site (left), the 3′ region of the *Il6* gene (centre), or the *Elam1* promoter (right) was assayed by PCR (ChIP). Data are representative of two independent experiments. **e**, Unstimulated or LPS-stimulated (10 ng ml^{-1}) peritoneal macrophages were immunoprecipitated with the indicated antibodies. The immunoprecipitated (IP) lysates were subsequently immunoblotted (IB) with anti-IκBζ.

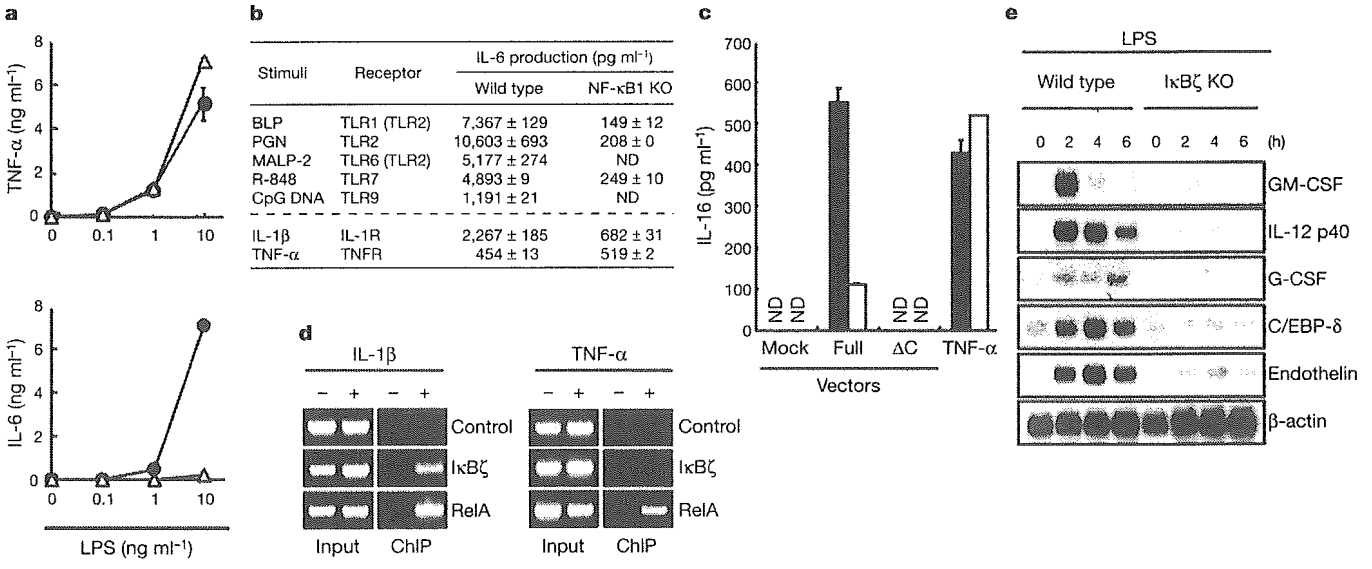

Figure 4 The TLR/IL-1R responses in NF-κB1/p50-deficient cells and microarray analysis of *IκBζ*$^{-/-}$ cells **a**, *NF-κB1*$^{+/+}$ (filled symbols) and *NF-κB1*$^{-/-}$ (open symbols) peritoneal macrophages were cultured with 10 ng ml^{-1} LPS in the presence of 30 ng ml^{-1} IFN-γ for 24 h. Values are means ± s.d. of triplicate experiments. **b**, *NF-κB1*$^{+/+}$ and *NF-κB1*$^{-/-}$ peritoneal macrophages and MEFs were cultured with 100 ng ml^{-1} BLP, 10 μg ml^{-1} PGN, 30 ng ml^{-1} MALP-2, 100 nM R-848, 3 μM CpG DNA, 10 ng ml^{-1} IL-1β or 10 ng ml^{-1} TNF-α in the presence of 30 ng ml^{-1} IFN-γ for 24 h. IL-1β- and TNF-α-induced IL-6 production were analysed by MEFs. Values are means ± s.d. of triplicate experiments. **c**, *NF-κB1*$^{+/+}$ (filled columns) and *NF-κB1*$^{-/-}$ (open columns) MEFs were retrovirally transfected with either the full-length (Full) or the deletion mutant (ΔC) of IκBζ. Furthermore, the same lines of untransfected cells were stimulated with 10 ng ml^{-1} TNF-α. Values are means ± s.d. of duplicate experiments. **d**, Chromatin from untreated (−), IL-1β-treated (left panel (+); 10 ng ml^{-1} for 3 h) or TNF-α-treated (right panel (+); 10 ng ml^{-1} for 3 h) wild-type MEFs were used for ChIP assays with the indicated antibodies. Precipitated DNA for the input (left) or the *Il6* κB site (right) was assayed by PCR. **e**, *IκBζ*$^{+/+}$ and *IκBζ*$^{-/-}$ peritoneal macrophages were stimulated with 10 ng ml^{-1} LPS for the indicated periods. Total RNA (5 μg) was extracted and subjected to northern blot analysis for expression of the indicated probes. GM-CSF, granulocyte-macrophage colony-stimulating factor; G-CSF, granulocyte colony-stimulating factor.

whether IκBζ promotes the ligand-induced activation of the *Il6* promoter, we introduced reporter plasmids containing the promoter of either *Il6* or *Elam1* (also known as *Sele*) into RAW 264.7 cells together with control or IκBζ expression vectors. LPS stimulation activated both the *Il6* and *Elam1* promoters in a dose-dependent manner. Under conditions of IκBζ overexpression, we found that the promoter activities of *Il6*, but not *Elam1*, were further enhanced (Fig. 3a). Ectopic expression of IκBζ alone also upregulated the activity of the *Il6* promoter in unstimulated cells (Fig. 3b). As an NF-κB binding site in the *Il6* promoter has been shown to have an important function in its activation, we transfected P19 cells with either a wild-type reporter or a mutant reporter in which the NF-κB binding site was disrupted[18]. IκBζ overexpression activated the wild-type reporter, but not the mutant NF-κB reporter (Fig. 3c). To probe directly the specific involvement of IκBζ in the κB site of the *Il6* promoter, we performed a chromatin immunoprecipitation assay (ChIP) to investigate the proteins bound to the region. In unstimulated cells, the NF-κB p50 subunit was readily detected in the *Il6* κB site as described previously[19]. On stimulation with LPS, RelA as well as p50 bound to the κB sites of the *Il6* and the *Elam1* promoter, but not the 3′ end of the *Il6* gene. In contrast, we found that IκBζ only bound to the *Il6* κB site, but not the other sites tested, in LPS-stimulated cells (Fig. 3d), demonstrating a specificity of IκBζ for the κB site in the *Il6* promoter. Finally, we addressed association of IκBζ with NF-κB family members. Immunoprecipitation analysis showed that IκBζ proteins interacted with p50, but not with RelA, RelB, c-Rel or the p52 subunit (Fig. 3e). These findings indicate that the positive effects by IκBζ may be exerted through association with the p50 subunit.

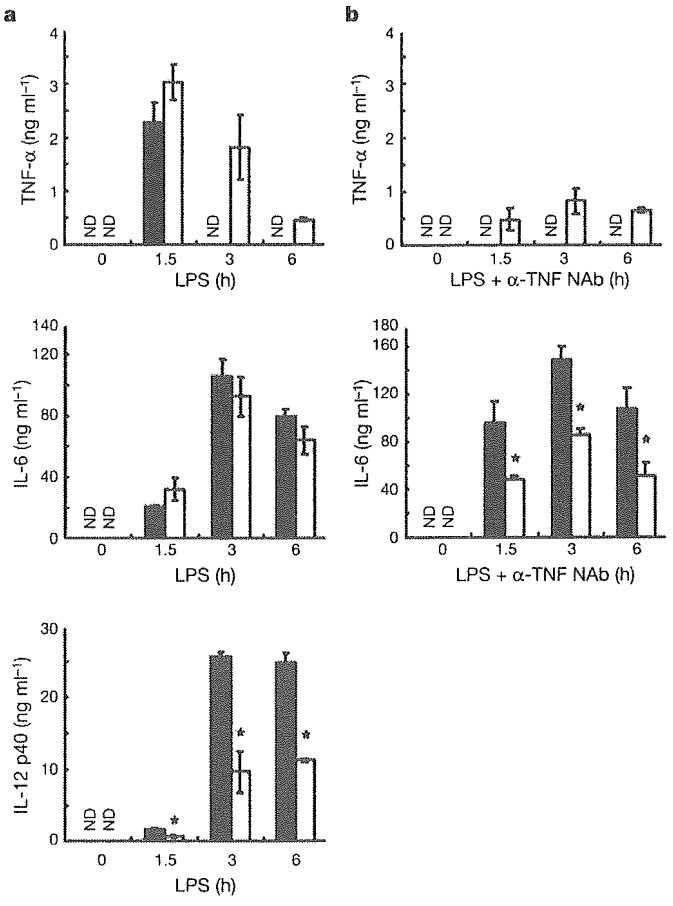

Figure 5 *In vivo* cytokine production in $I\kappa B\zeta^{-/-}$ mice. **a**, **b**, Age-matched $I\kappa B\zeta^{-/-}$ (open columns; $n = 3$ in **a** and 2 in **b**) and $I\kappa B\zeta^{+/+}$ (filled columns; $n = 3$ in **a** and **b**) mice were intraperitoneally injected with 1.5 mg LPS only (**a**), or with 10 μg anti-TNF NAb 1 h before the LPS injection (**b**). Sera were collected at the indicated times. Values are means ± s.d. of sera samples at the indicated times. Asterisk, statistical significance ($P < 0.05$) in a two-tailed Student's *t*-test comparing $I\kappa B\zeta^{+/+}$ and $I\kappa B\zeta^{-/-}$ mice.

The aforementioned results prompted us to study NF-κB1/p50-deficient cells. As previously reported, whereas LPS-induced TNF-α production in $NF\text{-}\kappa B1^{-/-}$ macrophages is normal, $NF\text{-}\kappa B1^{-/-}$ macrophages show defective LPS-induced production of IL-6 (refs 20, 21; see also Fig. 4a). Additionally, production of IL-6 in response to stimulation by IL-1 and other TLR ligands was severely impaired in $NF\text{-}\kappa B1^{-/-}$ cells (Fig. 4b). Thus, the TLR/IL-1R-mediated responses in $NF\text{-}\kappa B1^{-/-}$ mice are similar to those in $I\kappa B\zeta^{-/-}$ mice. We tested further whether IκBζ overexpression induced IL-6 production in $NF\text{-}\kappa B1^{-/-}$ cells. Compared with $NF\text{-}\kappa B1^{+/+}$ cells, IκBζ-mediated production of IL-6 was markedly reduced in $NF\text{-}\kappa B1^{-/-}$ MEFs, indicating that NF-κB1 is critical for the effect of IκBζ (Fig. 4c). Both IL-1 and TNF-α activate similar sets of signalling molecules such as NF-κB and mitogen-activated protein kinases, and culminate in IL-6 expression. However, signalling mediated by IL-1/TLR ligands, but not TNF-α, specifically recruited IκBζ to the *Il6* promoter (Fig. 4d), presumably accounting for the responsiveness difference between TLR/IL-1R and TNFR. Next, we searched for other LPS-inducible genes regulated by IκBζ using microarray analysis. Dozens of LPS-inducible genes were significantly affected by the IκBζ deficiency (Supplementary Fig. 4a). Several of them were subsequently tested by northern blot analysis for confirmation of accuracy. Among them, LPS-induced expression of granulocyte-macrophage colony-stimulating factor (*Csf2*), IL-12 p40 (*Il12b*), granulocyte colony-stimulating factor (*Csf3*), C/EBP-δ (*Cebpd*) and endothelin 1 (*Edn1*) was compromised in $I\kappa B\zeta^{-/-}$ macrophages (Fig. 4e). Indeed, time course northern blot analysis showed that the kinetics of LPS induction of these genes were similar to that for IL-6 rather than TNF-α (Fig. 2h, Supplementary Fig. 4b, and data not shown), further supporting the model of a two-step regulation of these genes in TLR/IL-1R signalling pathways. Regarding the relationship between the κB sequences of the genes tested and IκBζ requirement, the promoters of IκBζ-regulated genes contained distinct κB sequences. Therefore, it may be difficult to determine whether an arbitrary LPS-inducible gene is IκBζ-dependent through simple sequence comparison of the κB sites (ref. 22; see also Supplementary discussion 2 and Supplementary Fig. 4c–e).

Finally, we examined *in vivo* cytokine production after LPS injection. Although LPS-induced IL-12 p40 production was impaired, IL-6 production was almost normal in $I\kappa B\zeta^{-/-}$ mice. Surprisingly, $I\kappa B\zeta^{-/-}$ mice exhibited more prolonged TNF-α production than $I\kappa B\zeta^{+/+}$ mice (Fig. 5a). As TNF-α is a major IL-6 producer under conditions of endotoxin-induced shock, we next attempted to negate biological activities of TNF-α by prior treatment with anti-TNF-α neutralizing antibodies (anti-TNF NAbs) (ref. 23). In anti-TNF NAb-treated $I\kappa B\zeta^{-/-}$ mice the serum concentration of LPS-induced IL-6 was significantly reduced compared with anti-TNF NAb-treated $I\kappa B\zeta^{+/+}$ mice (Fig. 5b), demonstrating that the prolonged TNF-α production might compensate for impaired IL-6 production in $I\kappa B\zeta^{-/-}$ mice. The prolonged TNF-α production might be secondary to the loss of IκBζ-regulated factors that negatively modulate TNF-α production. Alternatively, IκBζ might act directly as a negative regulator for TNF-α production in certain cells. Although the molecular mechanism of the prolonged TNF-α production remains unknown, such prolonged TNF-α production might lead to development of the skin lesion in aged $I\kappa B\zeta^{-/-}$ mice as demonstrated in TNF-α-mediated inflammatory diseases occurring in other mouse models[24,25].

We provide genetic evidence that IκBζ is essential for TLR/IL-1R-mediated IL-6 production. As IκBζ itself is an inducible protein, TLR/IL-1R-mediated IL-6 expression may be regulated in a two-

step mechanism. Moreover, microarray analysis showed that IκBζ might control LPS-inducible genes other than *Il6*. Further analysis that clarifies the molecular basis of IκBζ-dependent gene expression will provide new insight into the TLR/IL-1R-mediated MyD88-dependent immune responses. □

Methods

Generation of $I\kappa B\zeta^{-/-}$ mice

Genomic DNA containing the *IκBζ* gene was isolated, as described previously[26]. We constructed the targeting vector by replacing a 2.0-kilobase (kb) fragment encoding the central portion of IκBζ with a neo^R cassette that was transfected into embryonic stem cells (E14.1). G418 and gancyclovir doubly resistant colonies were screened by polymerase chain reaction (PCR) and Southern blotting. We micro-injected two independent homologous recombinants into C57BL/6 blastocysts and intercrossed heterozygous F_1 progenies to obtain $I\kappa B\zeta^{-/-}$ mice. Mice from these independent clones displayed identical phenotypes. $I\kappa B\zeta^{-/-}$ mice and their wild-type littermates at the age of 6–12 weeks were used for the current studies. All animal experiments were conducted with the approval of the Animal Research Committee of the Research Institute for Microbial Diseases (Osaka University, Osaka, Japan).

Reagents and mice

LPS, PGN, MALP-2, flagellin, R-848 and CpG oligodeoxynucleotides were prepared as described previously[26]. Polyclonal antibody against IκBζ was obtained by immunizing rabbit with the C-terminal portion of the murine IκBζ protein. We used antibodies against phosphorylated ERK and JNK (Cell signalling), antibodies against ERK, JNK, p38, RelA, p50, c-Rel RelB, p52 (Santa Cruz), antibodies against RelA in ChIP assays (Biomol) and antibodies against murine TNF-α for neutralization (R&D). Recombinant TNF-α and IL-1β were obtained from Genzyme. NF-κB1/p50-deficient mice were as described previously[20].

Measurement of pro-inflammatory cytokine and NO

Thioglycollate-elicited peritoneal macrophages or MEFs were cultured as described previously[26]. Concentrations of TNF-α (Genzyme), IL-6 (R&D) and IL-12 p40 (Genzyme) in the culture supernatant were measured by an enzyme-linked immunosorbent assay according to the manufacturer's instructions. Concentrations of NO were measured by the Griess method according to the manufacturers' instructions (DOJINDO). To measure *in vivo* cytokine concentrations, sera were taken from $I\kappa B\zeta^{+/+}$ or $I\kappa B\zeta^{-/-}$ mice. Anti-TNF NAbs were reconstituted in PBS to 20 μg ml^{-1}, and 10 μg (500 μl) of the reagent was intraperitoneally injected 1 h before LPS injection.

Electrophoretic mobility shift assay

This assay was performed as described previously[26].

Plasmids and retroviral transfection

The reporter plasmids consisted of the 5′ flanking region (−1240/+40) of the murine *Il6* gene, and were used in Fig. 3a, b. The reporter plasmids used in Fig. 3c were as described previously[18,27]. The full-length or the deletion mutant IκBζ, which lacks the C-terminal portion (ΔC; ref. 4), was cloned into pMRX retroviral vector, and the transfection was performed as described previously[28].

Luciferase reporter assay

Reporter plasmids were transiently co-transfected into RAW 264.7 and P19 cells with either the control or IκBζ expression vectors using SUPERFECT transfection reagent (Qiagen). Luciferase activities of total cell lysates were measured using the Dual-luciferase reporter assay system (Promega) as described previously[29].

Chromatin immunoprecipitation assay

The ChIP assay was performed essentially with a described protocol (Upstate Biotechnology). 2×10^6 RAW 264.7 cells or 5×10^5 MEFs were stimulated with LPS (1 μg ml^{-1} for 3 h), IL-1β (10 ng ml^{-1} for 3 h) or TNF-α (10 ng ml^{-1} for 3 h), respectively. Precipitated DNAs were analysed by quantitative PCR (35–40 cycles) using primers 5′-CGATGCTAAACGACGTCACATTGTGCA-3′ and 5′-CTCCAGAGCAGAAT GAGCTACAGACAT-3′ for the κB site in the *Il6* promoter, 5′-GCAGATGGACTTAGC TCGTCTCATTCA-3′ and 5′-CCACTCCTTCTGTGACTCCAGCTTATC-3′ for a 3′ gene segment in the *Il6* promoter and 5′-GATGCAGTTGAGAATTTCCTCTTAGCC-3′ and 5′-TGGAATAGTTGTTCTGGCGTTGGATCC-3′ for the κB site in the *Elam1* promoter.

Western blot analysis and immunoprecipitation

Western blot was performed as described previously[26].

Gene chip analysis

Miroarray analysis (Affimetrix) using $I\kappa B\zeta^{+/+}$ and $I\kappa B\zeta^{-/-}$ peritoneal macrophages was performed as described previously[30]. The colour image for gene expression was generated by GeneSpring6.0 (Silicon Genetics) software.

Histological analysis

Tissues were fixed in 10% phosphate-buffered formalin, and paraffin-embedded tissue sections were stained with haematoxylin and eosin or PAS staining using standard techniques.

Received 1 April; accepted 7 June 2004; doi:10.1038/nature02738.

1. Takeda, K., Kaisho, T. & Akira, S. Toll-like receptors. *Annu. Rev. Immunol.* **21**, 335–376 (2003).
2. Janeway, C. A. Jr & Medzhitov, R. Innate immune recognition. *Annu. Rev. Immunol.* **20**, 197–216 (2002).
3. O'Neill, L. A. Therapeutic targeting of Toll-like receptors for inflammatory and infectious diseases. *Curr. Opin. Pharmacol.* **3**, 396–403 (2003).
4. Yamazaki, S., Muta, T. & Takeshige, K. A novel IκB protein, IκB-ζ, induced by proinflammatory stimuli, negatively regulates nuclear factor-κB in the nuclei. *J. Biol. Chem.* **276**, 27657–27662 (2001).
5. Kitamura, H., Kanehira, K., Okita, K., Morimatsu, M. & Saito, M. MAIL, a novel nuclear IκB protein that potentiates LPS-induced IL-6 production. *FEBS Lett.* **485**, 53–56 (2000).
6. Haruta, H., Kato, A. & Todokoro, K. Isolation of a novel interleukin-1-inducible nuclear protein bearing ankyrin-repeat motifs. *J. Biol. Chem.* **276**, 12485–12488 (2001).
7. Muzio, M., Ni, J., Feng, P. & Dixit, V. M. IRAK (Pelle) family member IRAK-2 and MyD88 as proximal mediators of IL-1 signaling. *Science* **278**, 1612–1615 (1997).
8. Wesche, H., Henzel, W. J., Shillinglaw, W., Li, S. & Cao, Z. MyD88: an adapter that recruits IRAK to the IL-1 receptor complex. *Immunity* **7**, 837–847 (1997).
9. Medzhitov, R. *et al.* MyD88 is an adaptor protein in the hToll/IL-1 receptor family signaling pathways. *Mol. Cell* **2**, 253–258 (1998).
10. Alexopoulou, L., Holt, A. C., Medzhitov, R. & Flavell, R. A. Recognition of double-stranded RNA and activation of NF-κB by Toll-like receptor 3. *Nature* **413**, 732–738 (2001).
11. Kawai, T. *et al.* Lipopolysaccharide stimulates the MyD88-independent pathway and results in activation of IFN-regulatory factor 3 and the expression of a subset of lipopolysaccharide-inducible genes. *J. Immunol.* **167**, 5887–5894 (2001).
12. Doyle, S. *et al.* IRF3 mediates a TLR3/TLR4-specific antiviral gene program. *Immunity* **17**, 251–263 (2002).
13. Ghosh, S. & Karin, M. Missing pieces in the NF-κB puzzle. *Cell* **109** (suppl.), S81–S96 (2002).
14. Zhang, G. & Ghosh, S. Molecular mechanisms of NF-κB activation induced by bacterial lipopolysaccharide through Toll-like receptors. *J. Endotoxin Res.* **6**, 453–457 (2000).
15. Janssens, S. & Beyaert, R. Functional diversity and regulation of different interleukin-1 receptor-associated kinase (IRAK) family members. *Mol. Cell* **11**, 293–302 (2003).
16. Eto, A., Muta, T., Yamazaki, S. & Takeshige, K. Essential roles for NF-κB and a Toll/IL-1 receptor domain-specific signal(s) in the induction of IκB-ζ. *Biochem. Biophys. Res. Commun.* **301**, 495–501 (2003).
17. Akira, S., Taga, T. & Kishimoto, T. Interleukin-6 in biology and medicine. *Adv. Immunol.* **54**, 1–78 (1993).
18. Matsusaka, T. *et al.* Transcription factors NF-IL6 and NF-κB synergistically activate transcription of the inflammatory cytokines, interleukin 6 and interleukin 8. *Proc. Natl Acad. Sci. USA* **90**, 10193–10197 (1993).
19. Zhong, H., May, M. J., Jimi, E. & Ghosh, S. The phosphorylation status of nuclear NF-κB determines its association with CBP/p300 or HDAC-1. *Mol. Cell* **9**, 625–636 (2002).
20. Sha, W. C., Liou, H. C., Tuomanen, E. I. & Baltimore, D. Targeted disruption of the p50 subunit of NF-κB leads to multifocal defects in immune responses. *Cell* **80**, 321–330 (1995).
21. Sanjabi, S., Hoffmann, A., Liou, H. C., Baltimore, D. & Smale, S. T. Selective requirement for c-Rel during IL-12 P40 gene induction in macrophages. *Proc. Natl Acad. Sci. USA* **97**, 12705–12710 (2000).
22. Hoffmann, A., Leung, T. H. & Baltimore, D. Genetic analysis of NF-κB/Rel transcription factors defines functional specificities. *EMBO J.* **22**, 5530–5539 (2003).
23. Hill, M. R. & McCallum, R. E. Identification of tumor necrosis factor as a transcriptional regulator of the phosphoenolpyruvate carboxykinase gene following endotoxin treatment of mice. *Infect. Immun.* **60**, 4040–4050 (1992).
24. Pasparakis, M. *et al.* TNF-mediated inflammatory skin disease in mice with epidermis-specific deletion of IKK2. *Nature* **417**, 861–866 (2002).
25. Douni, E. *et al.* Transgenic and knockout analyses of the role of TNF in immune regulation and disease pathogenesis. *J. Inflamm.* **47**, 27–38 (1995).
26. Yamamoto, M. *et al.* Role of adaptor TRIF in the MyD88-independent Toll-Like Receptor signaling pathway. *Science* **301**, 640–643 (2003).
27. Kinoshita, S., Akira, S. & Kishimoto, T. A member of the C/EBP family, NF-IL6 beta, forms a heterodimer and transcriptionally synergizes with NF-IL6. *Proc. Natl Acad. Sci. USA* **89**, 1473–1476 (1992).
28. Saitoh, T. *et al.* TWEAK induces NF-κB2 p100 processing and long lasting NF-κB activation. *J. Biol. Chem.* **278**, 36005–36012 (2003).
29. Toshchakov, V. *et al.* TLR4, but not TLR2, mediates IFN-β-induced STAT1α/β-dependent gene expression in macrophages. *Nature Immunol.* **3**, 392–398 (2002).
30. Kuwata, H. *et al.* IL-10-inducible Bcl-3 negatively regulates LPS-induced TNF-α production in macrophages. *Blood* **102**, 4123–4129 (2003).

Supplementary Information accompanies the paper on **www.nature.com/nature**.

Acknowledgements We thank T. Kitamura, A. Aderem, D. Golenbock and H. Tomizawa for providing Plat-E packaging cell lines, flagellin, the ELAM1 reporter plasmid, and R-848, respectively. We also thank T. Kawai and K. Ishii for discussions; M. Hashimoto for secretarial assistance; and N. Okita and N. Iwami for technical assistance. This work was supported by grants from Special Coordination Funds, the Ministry of Education, Culture, Sports, Science and Technology, Research Fellowships of the Japan Society for the Promotion of Science for Young Scientists, The Uehara Memorial Foundation, The Naito Foundation, and The Junior Research Associate from RIKEN.

Competing interests statement The authors declare that they have no competing financial interests.

Correspondence and requests for materials should be addressed to S.A (sakira@biken.osaka-u.ac.jp).

REVIEWS

TOLL-LIKE RECEPTOR SIGNALLING

Shizuo Akira and Kiyoshi Takeda‡*

One of the mechanisms by which the innate immune system senses the invasion of pathogenic microorganisms is through the Toll-like receptors (TLRs), which recognize specific molecular patterns that are present in microbial components. Stimulation of different TLRs induces distinct patterns of gene expression, which not only leads to the activation of innate immunity but also instructs the development of antigen-specific acquired immunity. Here, we review the rapid progress that has recently improved our understanding of the molecular mechanisms that mediate TLR signalling.

All living organisms are exposed constantly to microorganisms that are present in the environment and need to cope with invasion of these organisms into the body. The vertebrate immune response can be divided into innate and acquired immunity, with innate immunity being the first line of defence against pathogens. By contrast, acquired immune responses are slower processes, which are mediated by T and B cells, both of which express highly diverse antigen receptors that are generated through DNA rearrangement and are thereby able to respond to a wide range of potential antigens. This highly sophisticated system of antigen detection is found only in vertebrates and has been the subject of considerable research. Far less attention has been directed towards innate immunity, as it has been regarded as a relatively nonspecific system, with its main roles being to destroy pathogens and to present antigen to the cells involved in acquired immunity. However, recent studies have shown that the innate immune system has a greater degree of specificity than was previously thought and that it is highly developed in its ability to discriminate between self and foreign pathogens[1]. This discrimination relies, to a great extent, on a family of evolutionarily conserved receptors, known as the Toll-like receptors (TLRs), which have a crucial role in early host defence against invading pathogens[1,2]. Furthermore, accumulating evidence indicates that activation of the innate immune system is a prerequisite for the induction of acquired immunity, particularly for the induction of a T helper 1 (T_H1)-cell response[3,4]. This marked shift in our thinking has changed our ideas about the pathogenesis and treatment of cancers, and infectious, immune and allergic diseases. In the past few years, our knowledge of TLR signalling and the responses these receptors control has greatly increased. In this review, we discuss the TLRs, focusing on their signalling pathways.

**Department of Host Defense, Research Institute for Microbial Diseases, Osaka University, and ERATO, Japan Science and Technology Agency, 3-1 Yamada-oka, Suita, Osaka 565-0871, Japan.*
‡Department of Molecular Genetics, Medical Institute of Bioregulation, Kyushu University, 3-1-1 Maidashi, Higashi-ku, Fukuoka 812-8582, Japan.
Correspondence to S.A.
e-mail: sakira@biken.osaka-u.ac.jp
doi:10.1038/nri1391

TLR/IL-1R superfamily: structure and function

The discovery of the TLR family began with the identification of Toll, a receptor that is expressed by insects and was found to be essential for establishing dorsoventral polarity during embryogenesis[5]. Subsequent studies revealed that Toll also has an essential role in the insect innate immune response against fungal infection[6]. Homologues of Toll were identified through database searches, and so far, 11 members of the TLR family have been identified in mammals. The TLRs are type I integral membrane glycoproteins, and on the basis of considerable homology in the cytoplasmic region, they are members of a larger superfamily that includes the interleukin-1 receptors (IL-1Rs). By contrast, the extracellular region of the TLRs and IL-1Rs differs markedly: the extracellular region of TLRs contains leucine-rich repeat (LRR) motifs, whereas the extracellular region of IL-1Rs contains three immunoglobulin-like domains (FIG. 1a).

Toll/IL-1R domain. TLRs and IL-1Rs have a conserved region of ~200 amino acids in their cytoplasmic tails, which is known as the Toll/IL-1R (TIR) domain[7]. Within the TIR domain, the regions of homology comprise three conserved boxes, which are crucial for